AN ABSTRACT OF THE THESIS OF

William Friedkin for the degree of Master of Science in Horticulture presented on December 6, 1996.
Title: Digital Analysis of Remotely Sensed Images for Evaluating Color in Turfgrass

Abstract approved: _____
Timothy L. Righetti

Most conventional approaches to rating turf color for different turf varieties grown under similar conditions or for the same variety grown under different cultural conditions employ a visual subjective rating. By digitizing remotely sensed images acquired by use of a helium filled blimp and a Canon EOS camera, we were able to quickly and inexpensively rate turf plots. Our classification techniques evaluate histograms of pixels within a defined area rather than classifying each individual pixel as in traditional classifications. Analysis of the digital images includes separation of the image into the distinct 8-bit planes (red, green and blue). A plot map is created such that each experimental unit is defined by a rectangle. When this plot map is superimposed over the registered red, green and blue images, the respective histograms are collected for all plots. Data from these histograms are related to visual ratings for each plot. Supervised classification employs least squares regression equations developed from the histogram data and visual evaluations for the respective reference plots. Relationships apparent in the reference plots are used to predict values for all plots. Unsupervised classification is achieved by applying principal components transformation to the histogram data. The transformed values are then scaled to fit within the traditional 1 - 10 turf rating system by supplying maximum and minimum values. Supervised classifications produce predicted color values that are similar to visual ratings, but with greater statistical significance and fewer violations of the assumptions for ANOVA. Unsupervised classifications were similar to supervised classifications in two of three trials, but not consistently related to visual ratings in a third.

Digital Analysis of Remotely Sensed Images for Evaluating Color in Turfgrass

by

William Friedkin

A THESIS

submitted to

Oregon State University

in partial fulfillment of
the requirements for the
degree of

Master of Science

Presented December 6, 1996
Commencement June 1997

Master of Science thesis of William C. Friedkin presented on December 6, 1996

APPROVED:

Major Professor, representing Horticulture

Chair of Department of Horticulture

Dean of Graduate School

I understand that my thesis will become part of the permanent collection of Oregon State University libraries. My signature below authorizes release of my thesis to any reader upon request.

William Friedkin, Author

Acknowledgment

of

CONTRIBUTIONS FROM COOPERATORS

Dr. Timothy Righetti, my M.S. advisor provided input on experimental design and analysis. Dr. Tom Cook provided visual ratings of all turf plots for trials. Richard Matteson performed the image acquisition. The software macros for the percentile rank order transformation were written by Madrona Ludwig in Microsoft Excel.

TABLE OF CONTENTS

TABLE OF CONTENTS (Continued)

LIST OF FIGURES

LIST OF TABLES

Digital Analysis of Remotely Sensed Images for Evaluating Color in Turfgrass

INTRODUCTION

There is a subjective color association between 'greenness' and quality of different turf grass varieties or 'greenness' and efficiency of cultural practices such as fertilization in turf grass trials. Thousands of turf plots at research institutions throughout the world are visually rated for color and are placed on a scale from 1 to 9. Evaluators mentally average a variable spatial arrangement or variable color tone within a plot to formulate a color rating. Visually rating turf plots is tedious. Rating hundreds of plots requires a standardization that cannot be maintained from beginning to end. Most evaluators are only capable of whole number evaluations and violations of homogeneity of variance assumptions of ANOVA are common. An accurate and consistent evaluation procedure that produces statistically separable differences between experimental treatments is desired.

Traditional remote sensing techniques are generally too expensive and inconvenient for regular application in turfgrass research. Therefore, a system using remotely triggered cameras in a tethered blimp platform was developed. Color slides are then digitized for image analysis.

Digital color in this case is defined as a 24-bit color image with each color primitive (red, green and blue) displayed as an 8-bit image with 256 (2^8) brightness values. Each 8-bit color plane is characterized by a smoothed histogram with 256 brightness values on the X-axis and the frequency of occurrence on the Y-axis. The histogram characterization is a measure of the densities of all pixel brightness values within each plot. This characterization has been used traditionally as a probability density function within a maximum likelihood classification or as a statistical measure for a minimum distance to means classification. These are pixel by pixel classifications that average a pixel's

brightness value/density over a given area within each image and assignment is dependent on distribution about the mean.

Preliminary evaluations revealed that the mean or median values are often not as strongly correlated to visual color ratings as other points along red, green, or blue histograms. Therefore, a regression procedure was developed that could be used in place of minimum distance to means classification.

Histograms contain more information or spatial data than the mean, standard deviation, skewness and range. It is possible to assign lag points or building block locations that are relative to specific frequencies along the distribution of the curve. Lag point assignment is not dependent on statistical parameters and is therefore independent of the normal distribution restrictions that limit common classification schemes. The corresponding brightness values designated by the lag point definition from each of the three histogram characterizations provide for many user defined ratios and indices, such as the Normalized Difference Vegetative Indices (NDVI). The wide range of brightness values, ratios and indices calculated from different histogram processes can be used to make accurate regression predictions for all plots when combined with the visual ratings for the respective training sites.

When training site data or visual ratings are not available or are unreliable, an unsupervised classification would be appropriate. Because the relationship between visual ratings and characterizations is unknown, a principal component transformation is run on lag points from red, green, and blue histograms from each plot. The first principal component describes most of the data variability and can be rescaled to the range of values that best describes the accepted range for color quantification in turf plot rankings.

In this thesis, details on the tethered blimp camera system and histogram based predictions of turf color for both supervised and unsupervised classification schemes are described.

LITERATURE REVIEW

Introduction

Visual rating of turf plots is tedious. Rating hundreds of plots requires a standardization that cannot be maintained from beginning to end. Relative rankings may depend on the physical limitations of the evaluator to consistently quantify and differentiate similar colors. Like most turf researchers, we visually rate color on a scale of 1 to 9, with almost all plots falling within the range of 3 to 8. Logistic concerns limit most trials to three replications . This leads to violations of the assumptions for homogeneity of variance in ANOVA. Some plots have no variance (i.e. 7 - 7 - 7) and some plots have large variation between replications (i.e. 6 - 7 - 8). An accurate and consistent evaluation procedure that produces statistically separable differences between experimental treatments is desired.

Potential Uses of Remote Sensing in Turfgrass Evaluation

Remote sensing has been used as a crop management tool for many years (Toler et al., 1981; Wildman et al., 1983; Wildman et al., 1992; Everitt et al., 1993). Remote sensing techniques offer methods for determining rates of energy and chemical fluxes and rates of primary productivity, thus improving our understanding of bio-geochemical cycling (Botkin et al., 1984).

Although aircraft-based systems have long been successful in agronomic situations, they are prohibitively expensive, when daily or twice daily evaluations are required to document the rapid changes in color that can occur in turf varieties (Toler et al., 1981). Rapid deployment of the aircraft for measurement is difficult, dependent on the schedules of the pilot, and not easily scheduled with the changing physiological status of the turf. A tethered blimp may be an ideal photographic platform for turf evaluations. A

similar camera mounted blimp has been used to acquire large scale photography taken at low altitudes and to measure the dynamics of plant populations and the spatial relationships between vegetative components (Harris, N.R. et al, 1995). The blimp and photographic devices cost about $1200. One tank of helium (6.8 m^3) lasts six months. The entire system can be stored in ready to fly condition and photographs collected within minutes of the decision to take them. Daily evaluations are possible at a fraction of the cost of comparable aircraft systems.

Low-altitude, high-resolution photographs of turfgrass plots can be digitized and evaluated. Various approaches to analyzing photographs are possible. Analysis of aerial photographs depends on the type and complexity of photogrammetric procedures. Digital image analysis traditionally has made use of visual interpretation of color-infrared aerial photos to detect differences in biomass, color tone, or soil color (Wildman et al., 1992). Multispectral imagery has been used to detect stress vectors (Jackson and Gaston, 1994; Ribeiro et al., 1994), to assess foliar N status in forestry (Blinn, 1988), for chlorophyll and nitrogen levels in big leaf maple (Yoder and Crosby, 1995) and for measurement of *Botrytis fabae* incidence in bean fields (Malthus and Madiera, 1993).

Relationships Between Digital Information and Physiological Characteristics

Full color or Infra-Red photos can be easily digitized. After digitization, 24-bit images can be brought into a variety of software packages and separated into each of the 8-bit planes (red, green and blue). In most image analytical systems, each pixel can have a range of brightness values from 0 - 255 for each of the red, green and blue bands (Jensen, J.R., 1996). Therefore, each pixel is associated with a red, green, and blue value. Values of individual pixels or means of pixels from a defined area can often be related to physiological characteristics (Penuelas, J. et al 1994).

Regression has been used successfully for measurement of detectable nitrogen and chlorophyll content by reflectance in the green spectra and red edge for Douglas Fir

[*Pseudotsuga menziesii* (Mirb.) Franco.] (Dungan, J. et al., 1996). Variation in spectral data is caused by treatment. In this instance, the mean reflectance doubled at the high rate of fertilizer relative to the low treatment. Treatment effects on needle and canopy reflectance are significant in the visible region, most likely due to variation in chlorophyll as a response to the fertilizer treatments. Leaves from stressed plants (especially N limited) have higher reflectances in visible wavelengths and lower reflectances in the near infrared (Malthus, T.J. and Madiera, A.L. 1993).

Spectral Indices

Transformed values calculated from various mathematical expressions of individual color bands are often more diagnostic than single band information. It is not clear which expressions are most useful. A normalized difference vegetative index as defined below has often been especially useful (Wildman, W.E. et al., 1992; Jackson, P.L. and Gaston, G.G., 1994; Yoder, J.Y. and Crosby, R.E., 1995).

$NDVI = IR - R / (IR + R)$
IR = Near infrared pixel reflectance at 850 nm wavelength
R = Red pixel reflectance at 680 nm wavelength

A NDVI-like index was useful in distinguishing stress over the growing season. Several narrow-band indices provided better physiological information than NDVI. Specifically, the physiological reflectance index (PRI) followed changes in xanthophyll pigment concentrations and photosynthetic rates (Penuelas, J. et al 1994).

$PRI = G_{550} - G_{530} / (G_{550} + G_{530})$
G_{550} = Green pixel reflectance at the 550 nm wavelength
G_{530} = Green pixel reflectance at the 530 nm wavelength

The Normalized Pigment Chlorophyll Index (NPCI) varied with total pigment concentrations and chlorophyll. NPCI was found to be well correlated with chlorophyll content, carotenoid /chlorophyll *a*, lutein and neoxanthin/chlorophyll *a* (Penuelas, J. et al., 1993).

$NPCI = R_{680} - B_{430} / (R_{680} + B_{430})$
R_{680} = red pixel reflectance at the 680 nm wavelength
B_{430} = blue pixel reflectance at the 430 nm wavelength

The normalized difference between first derivative red and first derivative green (EFGN) index was found to be best correlated with chlorophyll over the other indices (Penuelas, J. et al., 1993).

$EFGN = dR_{700} - dG_{525} / (dR_{700} + dG_{525})$
dR_{700} = red pixel reflectance at the first derivative for the 700 μm wavelength
dG_{525} = green pixel reflectance at the first derivative for the 525 μm wavelength

Classification Schemes

Most classification schemes are pixel by pixel classifications that match pixel values to specific criteria. Criteria are usually defined by averaging pixel brightness values over a given area within an image.

Supervised classification is dependent on prior knowledge of evaluated plots or training sites. Parameters for class assignments are generated by applying statistical methods to training sites. Class assignment for pixels in unknown areas within the image are made according to specific criteria generated by the algorithm evaluating training sites.

In an unsupervised classification, unknown pixel assignments for all areas within the image are based on statistical and/or spectral patterns alone. The number of actual classes are defined before applying the classification algorithm. Because class assignment is limited by the number of possible classes, pixel assignment is driven by the statistical distribution of the spectral characteristics within the image and a class conditioned set of probabilities.

Computational Approaches to Classifying Regions within an Image

Spatial analysis of images and their relationships to other information rely on quantitative models (Dobson, J.E. 1993). Spatial quantifiers attempt to quantify the degree of spatial correlation and use this information together with the spectral response to decide class membership (Franklin, S.E. and B.A Wilson, 1992). For maximum likelihood, minimum distance to means, and simple discriminate analysis classifiers, homogeneity of pixel brightness values within training sites and a normal distribution of spectral reflectance curves in each of the color bands is assumed. More complex classification schemes use various approaches to deal with inconsistent variability within regions of an image.

Maximum Likelihood

The maximum likelihood classifier describes a spectral class by a probability distribution in multispectral (red, green and blue values) space. Such a distribution describes the chance of finding a pixel belonging to that class at any given location in multispectral space (Jensen, J.R., 1996). The position of pixel points in multispectral space can be described by vectors, whose components are the individual spectral responses in each band. Ratios of different spectral bands from the same image can be used to enhance subtle differences in spectral reflectance characteristics. This classification is strongly dependent on the normal distribution of brightness values (BV) within each of the color bands. By assuming that each histogram or probability function can be adequately approximated by a smooth curve, only the mean and variance for each class is needed for definition (Davis, S.M. et al., 1978). Because of this reduced control, unsupervised classification by maximum likelihood is not generally as effective. Mis-classified pixels may result from skewness of the distributions of pixel BVs' in the histogram. A viable alternative scheme is to note the set of pixel vectors corresponding to

a given class, using representative training data, then use these to classify the image by comparing unknown image pixels with each pixel in the training data until a match is found (Richards, J.A., 1986). Training data within the look-up table must contain one of every possible pixel vector for each class. Should some be missed, then corresponding pixels in the image would be left unassigned.

Minimum Distance to Means

Use of a mixture of three normal distributions or univariate distributions with three spectral bands provide better characterization for an area or class in a region than that in the unimodal distribution with one spectral band (Erol, H. and F. Akdeniz, 1995). Estimation parameters for class are limited to means for brightness for each band.

For a supervised classification, pixels in the photo scene exhibiting similar reflectance characteristics to the training site data are identified. Pixels that do not follow the defined statistical patterns remain unassigned. The acceptable range of values (distance from the mean) for each class is determined for all three bands. A pixel that has red, green, and blue values that fall within the appropriate ranges for a specific class is assigned to the appropriate category. Class means are calculated by using a methods of moments technique (Jensen, J.R., 1996). Method of moments is an estimation technique for means, variances and proportions in a mixture of two or more univariate normal populations. Each component is considered as a probability density function where components are arranged according to means. A Newton/Ralphson iteration (Jensen, J.R., 1996) is used for computing the starting values. The advantage of this classification scheme is that variables are defined between and/or within multiple band histogram characterizations rather than by a single component.

For an unsupervised classification, means and distances are not defined by training sites. Categories are defined by comparing pixels with their neighbors (adjacent pixels) to identify regions of similarity that can then be used to define mean and minimum distance

values for classification. (Jackson, P.L. and Gaston, P.L., 1994). Unclassified pixels are assigned to identified nearest neighboring peaks within the respective color band histogram (Jackson, P.L. and Gaston, P.L., 1994).

There is a non-parametric per pixel classifier, the first nearest neighbor rule (1-nn rule) that can be used with the minimum distance to means classifier (Hardin, P.J. and Thomson, C.N. 1992). Unlike the maximum likelihood classifier, the 1-nn classifier requires that the actual training vectors be stored in memory. In classification, an unknown pixel that falls into a polygon takes the label of the training pixel that 'owns' the polygon. The 1-nn rule is conceptualized as a classifier based on Thiessen polygons constructed around each of the training pixels. All pixels that do not contribute to the definition of the nearest neighbor rule boundary (a straight line) are eliminated or unassigned.

Statistical Pattern Recognition

In the statistical pattern recognition approach (statpr) or semantic approach, a set of characteristic measurements, denoted features, are extracted from the input data (training sites) and are used to assign features to appropriate classes. Features generated by a state of nature or class-conditioned set of probabilities and or probability density functions (Schalkoff, R., 1992). The maximum likelihood and minimum distance to means classifiers fall within this category.

The syntactic pattern recognition approach formulates hierarchical descriptions of complex patterns built from simpler sub-patterns (Schalkoff, R., 1992). Primitive elements or 'building blocks' are extracted from the input data. Histogram characterizations (including various histogram transformations) and resultant regression analysis, discriminate analysis and principle component analysis are syntactic recognition approaches that are used in conjunction with the semantic approach to increase the power of pattern recognition capabilities.

Discriminate Analysis

A fundamental function in pattern recognition is the discriminate function where the three dimensional feature space (red, green, and blue) is divided into different regions. The partitions become hyperplanes if the discriminate function is linear (Jain, A.K., 1989).

Discriminate analysis is used because it locates features that maximize the separation of the classes. The discriminate features are defined by the global mean, the mean pixel value (within class mean), the mean across all pixel/bands (between class mean) and probability. Pixels are classified based on discriminate functions that appropriately weight each red, green, and blue band.

Transforming Images and Extracting More Information

The maximum likelihood, minimum distance to means, and simple discriminate analysis procedures described above all assume homogeneity of pixel brightness values within training sites (or unsupervised grouping) and a normal distribution of spectral reflectance curves in each color band. This is rarely the case. Therefore, more complex classification schemes have evolved which are less dependent on assumptions of homogeneity or normality. The following approaches either provide more variables to evaluate, transform the original red, green, and blue values, or combine the information in multiple features.

Histogram Characterization

Within a defined area of an image (pixel window), one can obtain an occurrence frequency or histogram describing all pixels within the region. Feature selection processes can be more precise because frequency tables contain more spatial data for classification than mean, standard deviation, skewness and range (Gong, P. and Howarth,

P.J., 1992). The histogram or frequency table is an image characterization tool that can be applied to either entire images or segments of an image (Wehde, M.E., 1995).

The relative frequencies of spectral classes are measured within a moving window of pixels (kernel) (Lark, R.M., 1995a). Each pixel is allocated to a spectral class whose local neighborhood most closely corresponds the central pixel within a kernel is likely to belong to the same classification as the majority of its neighbors. This nearest neighbor classification requires that all conceptual or truth classes and spatial classes show a pattern or correspondence. Conceptual classes are made up from spectral classes whose relative frequencies have no significant difference. The conceptual classes are then 'truthed' for legend assignment.

Frequency based classifiers can be used with multiple brightness values from separate spectral bands. Original data is transformed to frequency based parameters that are used for a least squares fit with physical parameters such as the leaf area index and leaf reflectance (Qi, J. et al., 1995).

Percentile Transformed Histogram Values

There is a cumulative relationship for a pixel location in the frequency distribution. A pixel's value can be defined as its percentile position on the cumulative frequency distribution. A percentile rank ordering transformation will place pixels into proper perspective with respect to all other pixels (Wehde, M.E.,1995). Regardless of the original image data type and range, the output of the transformation is an image with rescaled values between 0 and 100. This transformation translates values from the horizontal axis into output pixel values on the vertical axis (f). In this way, values which are more numerous in the original image are spread apart while those that are less numerous are kept closer together. The axes can then be rescaled for processing of byte data or rescaled to a range of values for an unsupervised or supervised classification.

Log Transformed Histogram Values

Quantification from reflectance data for variability within the spectral band can be measured by logarithmic transformation of the histogram (Grossman, Y.L. et al., 1996). There is a high correlation between transformed histogram characterizations (2^{nd} derivative = 0) and nitrogen levels within the foliage when measured by multiple linear regression. Transformation of the histograms is a characterization that is non-empirical.

Standardizing Images

Images of the same scene often vary when taken at different times. Average intensity and the range of values for the bands being evaluated often change. For example, changes in values as one moves from one region to another vary in magnitude among similar images of the same scene.

Linear regression has been used for normalization in change detection. The regression equation (first-order polynomial equation) predicts what a given pixel's value would be if it had been acquired under the same condition as the reference scene. The equations are developed by matching pixel values from normalization targets present in both the scene to be normalized and the reference scene (Eckhardt, D.W. et al., 1990). In this case, regression models developed from a wide range of data values were generally better predictors than those developed from a smaller range of brightness values. The wider the range of BV values in the training site, the more accurate the regression prediction becomes.

Principle Component Analysis in Remote Sensing

Much of the information in multispectral images is redundant. Features are often correlated to each other. Principle component analysis creates a set of variables (eigenvectors) that contain original variability without redundancy.

The eigenvectors are used to discriminate similar spectra from distinct groups (Galvao, L.S. et al., 1995). The first eigenvector describes most of the data variability. This procedure is a transformation in which the new coordinate system's features are all uncorrelated (Jahne, B., 1993). The new features after transformation are linear combinations of the old features and are the eigenvectors of the covariance matrix. The corresponding eigenvalues are the variances. Principal component analysis can automatically apply a first order calibration to account for exogenous effects such as illumination, calibration, and atmosphere or albedo (Collins, J.B. and C.E. Woodstock, 1996). Descriminant analysis using variables derived from reflectance data, specifically the first 3 principal components, NDVI and other defined indices can yield clear separation of communities or classes (Penuelas, J. et al., 1993). The use of the first three principal components and various vegetative indices (as defined by the spectral signature file) can yield a clear definition in unsupervised classification.

Use of principal components can refine the classification procedure. Pixel values can be replaced with principle components. Any of the principle components can then be subjected to traditional classification schemes (Baker, J.R. et al., 1991). After a minimum distance to means classification or a maximum likelihood classification, a linear stretch was performed on the principal components axes (from all 3 bands) in which 1% of the lower and upper extremes are clipped. This decorrelation scaling produced an image which fills the color space more fully (Baker, J.R. et al., 1991).

The sum of the products of eigenvectors or factor loadings and brightness values of a particular pixel within each of the color bands can also be used to assign a new BV to a specified pixel (Jensen, J.R., 1996). Ambiguous brightness values are eliminated in this principal component transformation. Each pixel would have a distinct and separate value under the respective 'principal component'. When placed in the blue, green, and/or red image plane, a principal component color composite is created.

Fuzzy Theory

There is some evidence that less rigid classification schemes may be more accurate. A pixel cannot be classified with 100% certainty. A one pixel in one class membership (hard partition) loses information. (Wang, F., 1990). Fuzzy set theory allows partial and multiple membership on a per pixel classification.

A fuzzy set does not have sharply defined boundaries. A fuzzy set B in X is characterized by a membership function f_B, which associates with each x a real number (0,1). The $f_B(x)$ represents the percentage of membership of x in B. The closer the value of $f_B(x)$ is to 1, the more x belongs to B (Zadeh, L.A., 1965). In calculating a fuzzy mean and a fuzzy covariance matrix, how much a pixel belongs to a class determines how much it contributes to the mean and covariance matrix of that class. In calculating a fuzzy mean, a sample pixel vector is multiplied by its membership grade or function before being added to the sum. In calculating a fuzzy covariance matrix for a class, the fuzzy covariance is multiplied by the membership grade or function before being added (Wang, F., 1990). In this way, fuzzy classification takes on the characteristics of a maximum likelihood classification as discussed earlier. A pixel's class membership is defined by its relationship to multiple mean vectors, which in turn must have some relationship to one another.

Chapter 3

COMPUTER ENHANCED TURF COLOR EVALUATIONS USING AERIAL PHOTOGRAPHY FROM A TETHERED BLIMP

William Friedkin

To be submitted to *Journal for the American Society of Horticulture*,
with Richard Matteson, T.L. Righetti, and Tom Cook as co-authors

Abstract

DIGITAL ANALYSIS OF REMOTELY SENSED IMAGES FOR EVALUATING COLOR IN TURFGRASS

William Friedkin

Rating turf color for different turf varieties grown under similar conditions or for the same variety under different cultural practices is difficult. Most conventional approaches employ a visual subjective rating. We have been using a tethered 5.1 m^3 blimp and a Canon EOS Rebel camera with a 28 mm lens to acquire images from various film types. A smaller balloon equipped with a Nikon 28mm single focal length point and shoot camera has also been used. Our current standard evaluation process is described. The blimp is tethered by 100 lb. test monofilament line or braided nylon cord. The camera is mounted on a gimbaled frame to maintain a vertical orientation. Radio controlled servos are used to rotate the platform and trigger the shutter. Slides are digitized in 24-bit tiff or bmp format. Analysis of the digital images includes separation of the image into the distinct 8-bit planes (red, green and blue). A plot map is created such that each experimental unit is defined by a rectangle. When this plot map is superimposed over the registered red, green and blue images, the respective histograms are collected for all plots. Data from those histograms are then related to visual ratings for each plot. The best fit linear relationship is used to predict a new rating. Predicted values (computer enhanced visual ratings) have the same general trends as the original ratings, with greater statistical significance and fewer violations of the assumptions for ANOVA.

Introduction

Visual rating of turf plots is tedious. Rating hundreds of plots requires a standardization that cannot be maintained from beginning to end. Relative rankings may depend on the physical limitations of the evaluator to consistently quantify and differentiate similar colors. Like most turf researchers, we visually rate color on a scale of 1 to 9, with almost all plots falling within the range of 3 to 8. Logistic concerns limit most trials to three replications . This leads to violations of the assumptions for homogeneity of variance in ANOVA. Some plots have no variance (i.e. 7 - 7 - 7) and some plots have large variation between replications (i.e. 6 - 7 - 8). An accurate and consistent evaluation procedure that produces statistically separable differences between experimental treatments is desired.

Remote sensing has been used as a crop management tool for many years (Toler et al., 1981; Wildman et al., 1983; Wildman et al., 1992; Everitt et al., 1993). Although aircraft-based systems have long been successful in agronomic situations, they are prohibitively expensive, when daily or twice daily evaluations are required to document the rapid changes in color that can occur in turf varieties (Toler et al., 1981). Rapid deployment of the aircraft for measurement is difficult, dependent on the schedules of the pilot, and not easily scheduled with the changing physiological status of the crop in the study. A tethered blimp may be an ideal photographic platform for turf evaluations. A similar camera mounted blimp has been used to acquire large scale photography taken at low altitudes and to measure the dynamics of plant populations and the spatial relationships between vegetative components (Harris, N.R. et al, 1995). The blimp and photographic devices cost about $1200. One tank of helium (6.8 m^3) lasts six months. The entire system can be stored in ready to fly condition and photographs collected within minutes of the decision to take them. Daily evaluations are possible at a fraction of the cost of comparable aircraft systems.

Analysis of aerial photographs depends on the type and complexity of photogrammetric procedures. Digital image analysis traditionally has made use of visual interpretation of color-infrared aerial photos to detect differences in biomass, color tone, or soil color (Wildman et al., 1992). Multispectral imagery has been used to detect stress vectors (Jackson and Gaston, 1994; Ribeiro et al., 1994), to assess foliar N status in forestry (Blinn, 1988), for chlorophyll and nitrogen levels in big leaf maple (Yoder and Crosby, 1995) and for measurement of *Botrytis fabae* incidence in bean fields (Malthus and Madiera, 1993).

Transformed values calculated from various mathematical expressions of individual color bands are often more diagnostic than single band information. It is not clear which expressions are most useful. A normalized difference vegetative index as defined below has often been especially useful (Wildman et al., 1992; Jackson and Gaston 1994; Yoder and Crosby, 1995).

NDVI = IR - R / (IR + R)
IR = near infrared pixel reflectance at 850 nm wavelength
R = red pixel reflectance at 680 nm wavelength

Leaves from stressed plants (especially N limited) have higher reflectances in visible wavelengths and lower reflectances in the near infrared (Malthus and Madiera,1993). A NDVI-like index applied to green wavelengths was useful in distinguishing stress over the growing season (Penuelas et al., 1994). Several narrow-band indices provided better physiological information than NDVI. Specifically, the physiological reflectance index (PRI) followed changes in xanthophyll pigment and photosynthetic rates.

$PRI = G_{550} - G_{530} / (G_{550} + G_{530})$
G_{550} = green pixel reflectance at the 550 nm wavelength
G_{530} = green pixel reflectance at the 530 nm wavelength

The Normalized Pigment Chlorophyll Index (NPCI) described below varied with total pigments and chlorophyll. NPCI was found to be well correlated with chlorophyll content, carotenoid /chlorophyll *a*, and neoxanthin/chlorophyll *a* (Penuelas et al., 1993).

$NPCI = R_{680} - B_{430} / (R_{680} + B_{430})$
R_{680} = red pixel reflectance at the 680 nm wavelength
B_{430} = blue pixel reflectance at the 430 nm wavelength

The normalized difference between first derivative red and first derivative green (EFGN) index was found to more strongly correlated with chlorophyll than other indices (Penuelas et al., 1993).

$EFGN = dR_{700} - dG_{525} / (dR_{700} + dG_{525})$
dR_{700} = red pixel reflectance at the first derivative 700 nm wavelength
dG_{525} = green pixel reflectance at the first derivative 525 nm wavelength

It is obvious that there are many ways to express digital data. Our objective in this presentation was to extract pixel information from color, false color IR, or other images using various film and filter combinations, and relate it to visual quantification. We allow the user to find the best fit linear relationship among either the raw data or any transformation or indices one chooses to evaluate. This relationship can then be used to predict new ratings for every plot. Our hypothesis was that computer enhanced visual ratings would be more accurate and statistically robust than the original visual ratings.

Materials and Methods

Blimp, Balloons, Cameras, Lenses, Filters, Film and Development

We have used a camera box suspended from a 5.1 m^3 helium filled blimp that can hold and operate one or two cameras (Fig. 3.1). The box contains a Canon EOS 35mm camera, fitted with either a Sigma 28 mm (f/1.8) lens or a Canon 15m (f/2.8) fisheye lens. It has been possible to mount a second camera within the box in such a way as to photograph the same scene with more than one film type at the same time. Focus is manually set to infinity. Shutter speed and aperture are automatically controlled by the camera for most film types.

Fishing swivels allow the platform to rotate freely. A small propeller is mounted on the box for manual orientation. Radio controlled servos, transmitters, and receivers are

used to control the propeller for orientation and for shutter operation. The blimp is flown between 61 and 122 meters above the turf plots, located at Oregon State University's Lewis Brown Farm in Corvallis, Oregon. Altitude is determined by referencing marks on the tether. Total weight of the box with cameras, servos, receivers and propeller is 2 kg.

We also use a smaller cross mount platform suspended from a 2.3 m^3 round balloon that can hold and operate one camera. The cross mount platform holds a Nikon LiteTouch 28mm single focal length, automatic focus, automatic shutter speed, point and shoot camera. The entire assembly including camera, servos, receivers, and propeller weighs 800 grams (Fig. 3.2). Although this system has less flexibility than the larger two camera system (ISO automatically defaults to 100), similar quality color and false color IR images can be obtained. Film, camera settings and filter choices are more limited with the smaller camera system. However, the No. 12 Wratten gelatin filter can be taped over the lens for False Color IR film. The 2.3 m^3 balloon system is less stable under windy conditions but is much less expensive and is still manageable on calm days.

We have experimented with Kodak Ectachrome 100, Fuji 50 ISO Velvia, Fuji 100 ISO Provia, Kodak Technical Pan, Kodak IR, Kodak False Color IR and Hyper-sensitized Technical Pan films (Microfluor LTD.). When using the IR films, a No.12 screw mounted filter is used. A Kodak No. 97, No. 73, or No. 89B Wratten gelatin filter can be used with Hyper-sensitized Technical Pan film.

Since the Technical Pan film has sensitivity to the 700 nm wavelength and the N. 97 or No. 89 filters eliminate wavelengths less than 690 nm, this combination gives a usable 10 nm (660 - 670) band image if photographed on a sunny, still day with a f/1.8 aperture and a 1/30 shutter speed. Use of the No. 73 filter consistently produces a 560 to 610 nm image with a f1.8 aperture and a 1/60 shutter speed.

DX coded ISO settings and automatic shutter speed and aperture were used for Kodak Ektachrome and Fuji film types. A manually set ISO of 25 and 100 with automatic shutter speed and aperture were used for Kodak Technical Pan and Kodak False Color IR

film. On very sunny days, an ISO of 200 is used for False Color IR film. A shutter speed of 800 and aperture of 13.0 is used for Kodak IR film.

Ektachrome and Fuji slide films were locally developed using the standard E4 process. False color IR film was commercially developed (HAS Images, Inc.) using the E6 film process. Technical Pan film was locally developed using the Technidol process. Hyper-sensitized Technical Pan and Kodak IR film were developed in our own dark room in Kodak HG-110 developer with a 26:214 developer:water ratio for 12 and 6 minutes, respectively.

Figure 3.1 The helium filled blimp and camera mounted platform

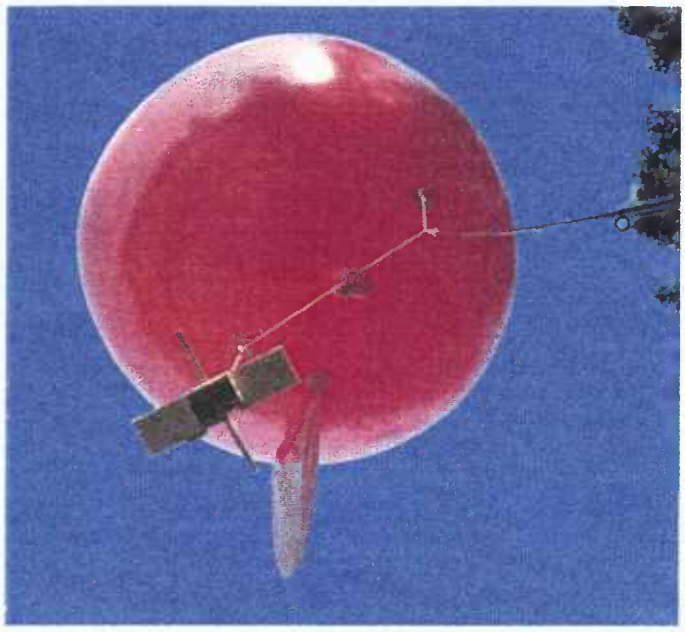

Figure 3.2 A helium filled balloon with camera on a cross mount platform

Comparative Color Evaluations

Hundreds of evaluations have been made over the last four years using various film types on a wide range of fertilizer and variety trials. All color ratings in the OSU turf program are currently being computer quantified. We routinely use a single camera system with Fuji Velvia or Provia film for the Canon and Minolta cameras, respectively. The following example demonstrates the process in what has become our standard evaluation procedure.

This study described below was designed to rate fertilizer efficiency/response through visual color ratings on ryegrass turf and to compare these results with a computer-assisted visual evaluation using Fuji ISO 50 Velvia film.

The study area measures 12.8 meters long by 12.2 meters wide. The turf trial consists of sixty - 1.2 m by 1.5 m plots. They are arranged in 6 rows - 10 plots long. Each plot is surrounded by a 7.6 cm wide herbicide strip. Rows are either 1.2 or 0.6 m apart (Fig. 3.3). The turf trial consists of three replications in a randomized complete block

design. There are 20 treatments; nine fertilizer sources at two rates (.0048 and .0096 kg • m^2 N), one fertilizer source at a single rate and the control. The treatments for each replication are described below:

Plot	Formulation	Rate
1	IBDU 100%	.45 kg N/ 93 m^2
2	PCU 100%	.45 kg N/ 93 m^2
3	IBDU 75%, PCU 25%	.45 kg N/ 93 m^2
4	IBDU 50%, PCU 50%	.45 kg N/ 93 m^2
5	IBDU 25%, PCU 75%	.45 kg N/ 93 m^2
6	24-4-12	.45 kg N/ 93 m^2
7	IBDU 100%	.90 kg N/ 93 m^2
8	PCU 100%	.90 kg N/ 93 m^2
9	IBDU 75%, PCU 25%	.90 kg N/ 93 m^2
10	IBDU 50%, PCU 50%	.90 kg N/ 93 m^2
11	IBDU 25%, PCU 75%	.90 kg N/ 93 m^2
12	24-4-12	.90 kg N/ 93 m^2
13	Turfgo 21-4-16	.45 kg N/ 93 m^2
14	Turfgo 21-4-16	.90 kg N/ 93 m^2
15	ESN 2003 MINI	.45 kg N/ 93 m^2
16	ESN 2003 MINI	.90 kg N/ 93 m^2
17	POLY-S 25-3-9	.45 kg N/ 93 m^2
18	POLY-S 25-3-9	.90 kg N/ 93 m^2
19	ESN 2003 reg.	.90 kg N/ 93 m^2
20	UNFERTILIZED CHECK	

Abbreviations are as follows:

Vigoro Industries, Inc.:

IBDU	= Isobutylidene diurea 31-0-0
PCU	= Experimental polymer-coated urea
24-4-12	= N source - 50% urea 50% IBDU (24N-1.7P-10K)

United Horticultural Supply :

Turfgro 24-4-16	= N source 50% urea 50% ESN (24N-1.7P-13.3K)
ESN 2003 MINI	= 100% resin-coated urea 43-0-0 small prill
ESN 2003 Reg.	= 100% resin-coated urea 43-0-0 large prill

O.M. Scott Co.:

POLY-S 25-3-9	= Polymer-coated, sulfur coated urea 40-0-0 (25N-1.3P-7.5K)

Visual color and computer-assisted color ratings were both analyzed by ANOVA with mean separation by LSD. A Bartlett test was conducted to evaluate assumptions concerning homogeneity of variance. Since design was not a complete factorial, it was analyzed with two different approaches. The experiment was evaluated both as 20 treatments with three replications and as a factorial experiment (treatments 1 - 5 and treatments 7 - 11) with 5 formulations at two rates.

The plots were visually rated and photographed on the same day. Three dates (6/26/95, 7/10/95 and 7/18/95) are treated as separate trials for comparison of visual and computer-assisted visual evaluations.

Computer-Assisted Visual Evaluations

Full color photographs were processed into slides. The 35mm slides in this example were scanned with a Polaroid Sprintscan into 24-bit color images in .bmp (bitmap) format. Negatives of other image types can also be scanned. Any slide or negative can be sent to commercial photo processing laboratories and converted to digital format on a

Kodak CD. The pcd format on CDs is converted to 24-bit color bmp (bitmap) format for further analysis.

We have decided on an approximately 650 x 650 pixel spatial resolution as a compromise between increasing resolution and manageable storage and processing size. Although up to 4000 x 6000 pixel resolution is possible, we have found few advantages to using greater resolution that requires longer computer processing times with increasing storage problems.

Easy Image and Field Notes software (Penmetrics Software, Corvallis, OR) are used to process the digital images. The software runs on standard Windows equipped 386 or 486 compatible computers with at least 8 megabytes of Random Access Memory. Steps in digital processing are as follows:

1) The scaled drawing (Fig. 3.3) is oriented north and south and plot corners are located as control points. The .dxf (drawing exchange file) drawing has two layers. The first layer is the outline of the plots. A second layer consists of horizontal lines in each plot. The order in which these lines are drawn is associated with the row number of the previously obtained visual ratings. Visual ratings are on a scale of 1 to 9 and are entered into a tab delimited .txt file with each entry in a separate, numbered row. The plots are ordered west to east along the row, consecutively north to south between rows.
2) After digitization, 24-bit images (Fig. 3.4) are brought into Easy Image and separated into each of the 8-bit planes (red, green and blue). The operator chooses one of the bands (usually the green) and using a thresholding routine, creates a mask (Fig. 3.5) to remove either shadows or bare spots from the photograph.
3) The mask 'image' is applied to each of the three bands - red, green and blue (Fig. 3.6). Masked pixels are given a value of zero. These pixels will be ignored in subsequent analysis.

4) The three thresholded bands are then georeferenced to the scaled drawing (Fig. 3.7). The size of the plot borders in the drawing (15 cm) is large enough that rectification need not be perfect. In this example, pixel size is 23 cm^2 .

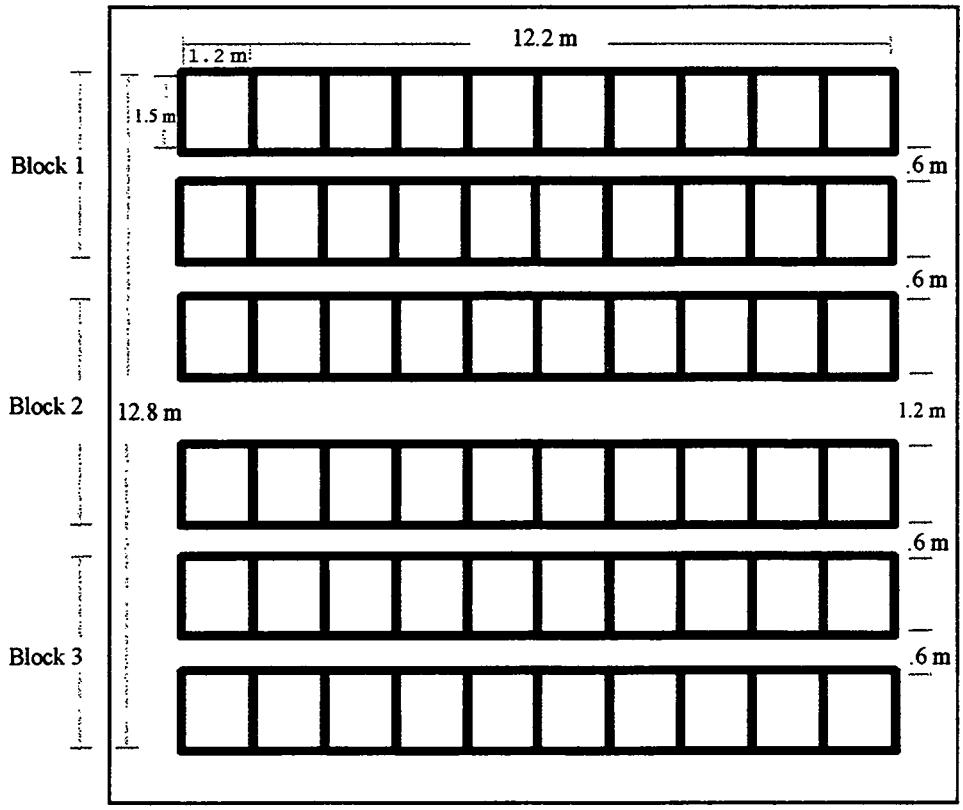

Figure 3.3 A scaled drawing of a fertilizer trial, oriented North to South

Figure 3.4 A remotely sensed, digital 24-bit image of the turf plots

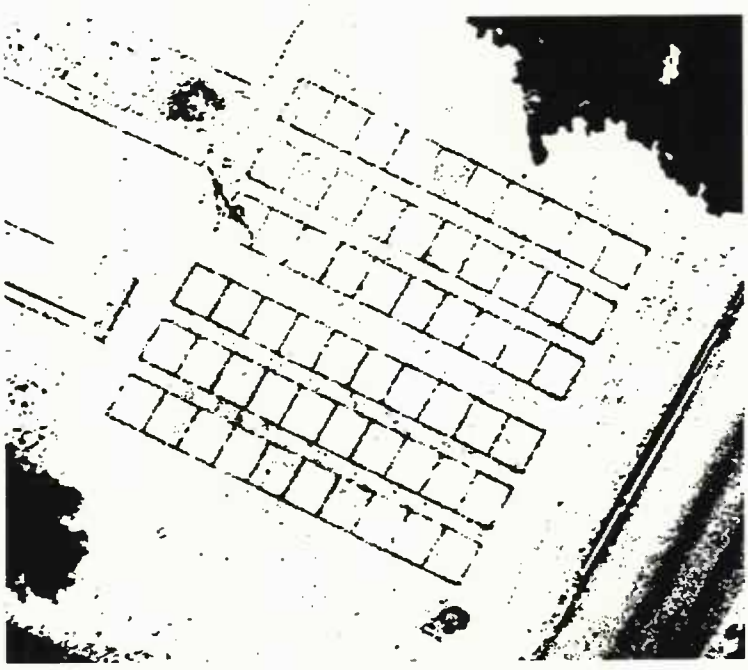

Figure 3.5 A black and white mask of the image, used to remove shadow and plot outlines from analysis

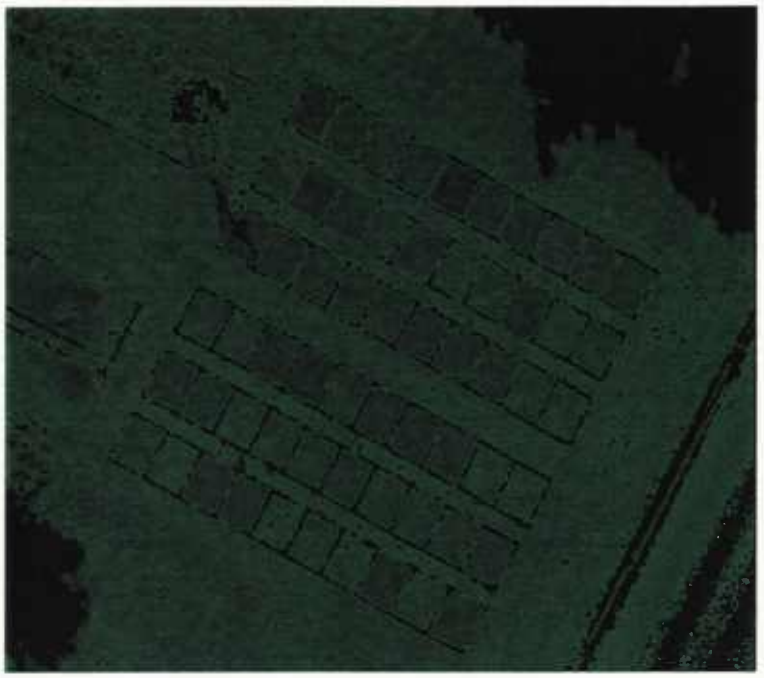

Figure 3.6 The green band of the image with mask applied

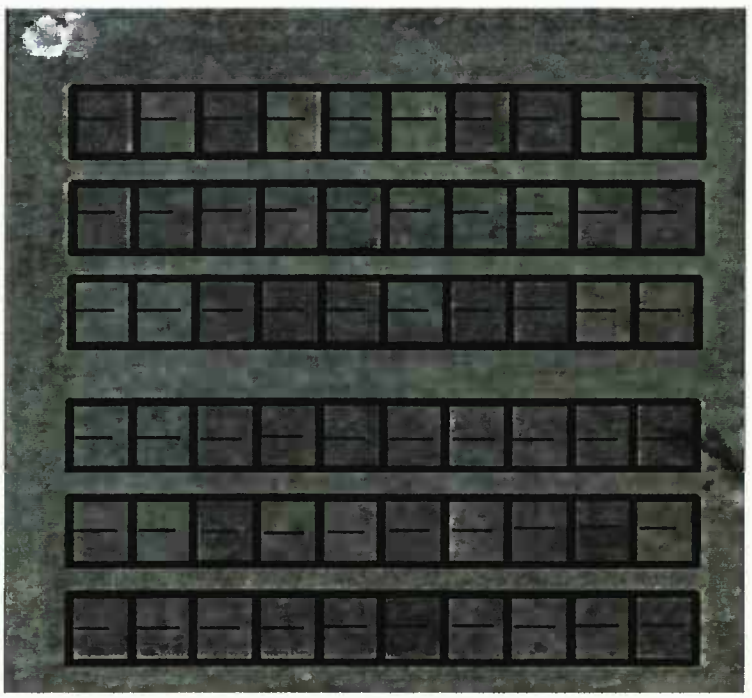

Figure 3.7 A rectified image that has been geocoded for placement on drawing with a second layer that identifies and selects plots in order of analysis

5) The software calculates a histogram for each of the three color bands for each plot as defined by the grid drawing (Fig. 3.8). Frequency of occurrence (f)is plotted along the vertical axis with individual measurements of pixel intensity between 0 and 255 along the horizontal axis. The raw histogram data is shown. The user can choose any degree of smoothing desired to produce smoothed histograms that are then used to extract x and y data points that describe the histogram. The median pixel value for a given frequency distribution was considered a mid-range value. Our software gives the user up to eight additional histogram positions to choose from.

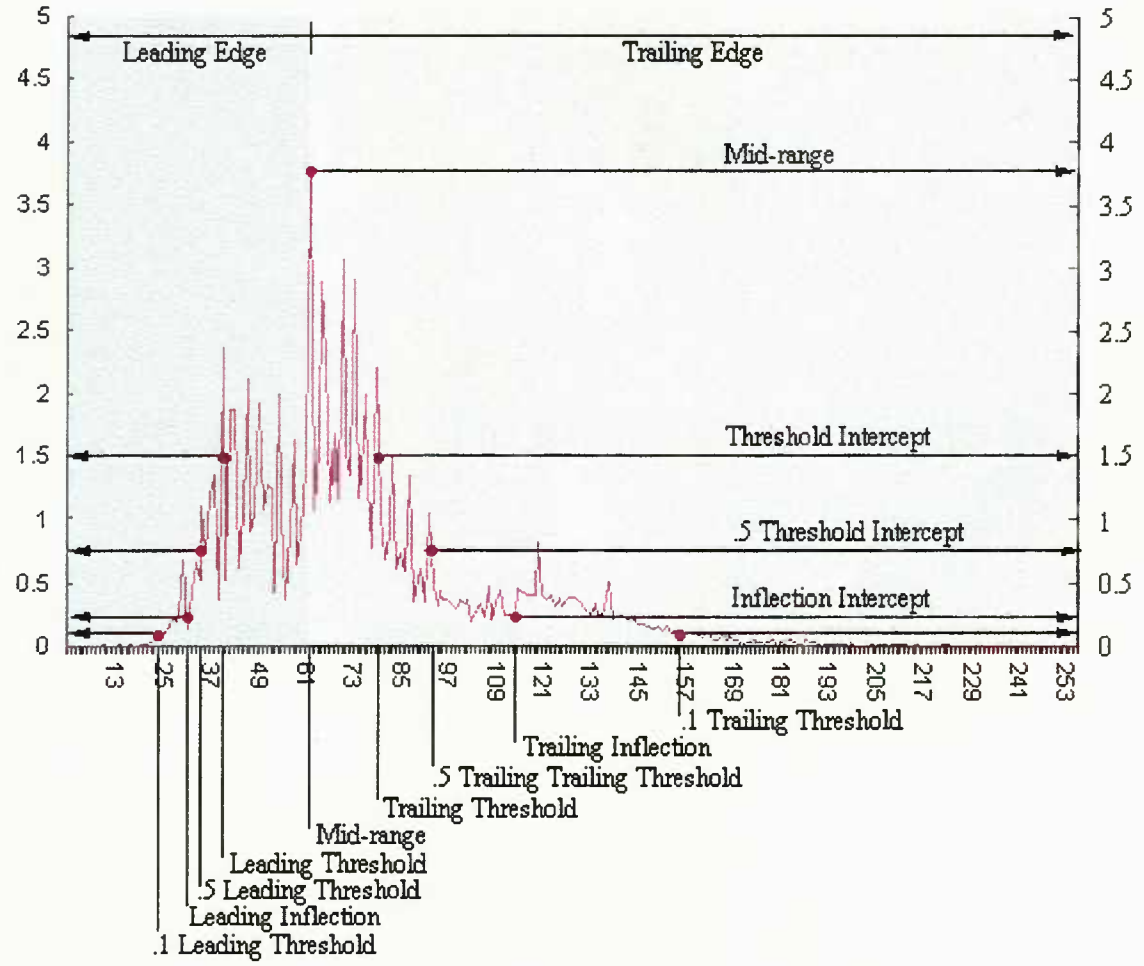

Figure 3.8 The 9 points used to characterize the respective histogram from each plot and their associated intercepts.

Any threshold *f* value can be chosen by the user to identify points on either the leading or trailing edges of the histogram. The automatic default is 1.5%. Pixel brightness (BV) ratings for *f* values 0.5 and 0.1 of the selected threshold are also automatically calculated and stored for both leading and trailing edges of the histogram (Fig. 3.8). Leading and trailing inflection points (2^{nd} derivative equals 0) are also located on the histogram.

Traditional indices are dependent on mid-range values within the respective spectral bands. Indices can also be calculated using values from any position on a histogram. With multiple points along each of the three color planes (red, green and blue), it is possible to have multiple user defined indices within and between the color and/or IR bands (i.e. Mid Red -Mid Green / (Mid Red + Mid Green), etc.). It is also possible to calculate various measures of variability within each plot (i.e. Red Trailing Inflection, Red Leading Inflection, etc.) With 27 values extracted from the original histograms and various user specified ratios and indices calculated from those values, we generate between 60 and 100 color variables describing each plot. Linear regression equations between these color variables and visual ratings are calculated and presented in order of decreasing R^2 values (Fig. 3.9). The user specifies the desired equation to produce a predicted rating for all the plots within the trial.

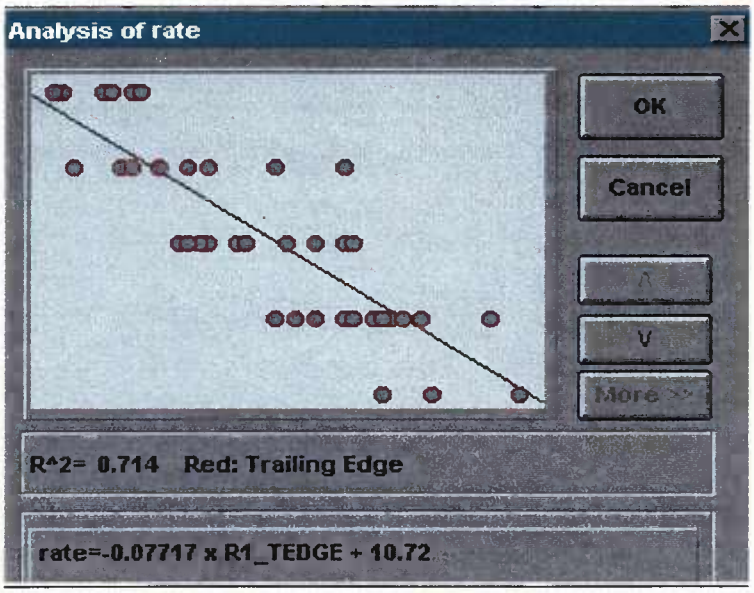

Figure 3.9 A regression between visual ratings and the red trailing edge histogram characterizations

Results and Discussion

The result of a regression between visual ratings and the best fit histogram characterization (Fig. 3.9), demonstrates the difficulties in making whole number evaluations. There are many instances of overlap in successive ratings. Median values are as expected but there are difficulties in consistently assigning values. An example of this may be a value between 5 and 6, where a 5 or a 6 is assigned according to a judgment call or when a visual assignment of 6 could possibly be 7 or 5.

The inability to assign the appropriate visual color value leads to violations of the assumptions for homogeneity of variance (Tables 3.1 and 3.2). Some plots (i.e. replicates of 7,7,7) have no variance where others (i.e. replicates of 6,7,8) have large variances. These violations can portray significant statistical differences when there indeed are none. Computer enhanced visual ratings did not violate assumptions of homogeneity of variance (Table 3.2). Bartlett test values were .698, .327, and .972 for computer assisted ratings while significant at levels less than .001 for visual evaluations on all three dates.

The computer detected significant differences in replication, treatment and rate in all three trials.

In randomized complete block design, significant differences among blocks increases the ability to detect possible treatment differences. Block effects were not detected with visual evaluations. Significant differences in the rate effect were also not detected in visual ratings for Trial 2. The detection of significant differences for computer ratings were consistent with visual ratings in their ability to detect treatment effect.

The mean square error is approximately 2 ½ times greater in the visual ratings than in computer-assisted ratings (Tables 3.1 and 3.2). A comparison of the coefficients of variation indicates there are 3.7, 3.1, and 2.4 times more variability among plots within treatments for visual ratings than in computer assisted ratings for trials 1, 2, and 3 respectively (Table 3.3). There is always a higher level of significance for treatment differences in the computer-assisted ratings and a higher level of significance for rate in 2 of 3 trials.

Both visual and computer assisted ratings resulted in similar relative rankings of treatments (Table 3.3). Computer assisted and visual ratings were also related to each other with slopes of approximately 1 and intercepts of approximately 0. These results imply that while computer-assisted evaluations are more precise than visual ratings, they quantify the same visual components that experienced evaluators utilize.

Our procedures differ from traditional minimum distance to means classifications. It is possible to traditionally classify pixels in an image and average classifications within each rectangle. However, we feel our regression approach is theoretically superior for several reasons. Mean values of red, green, and blue color bands are often not as strongly related to visual ratings as other points on their histograms. Various indices calculated from the histogram data can also be more strongly related to visual ratings than the means of the color bands. Furthermore, visual ratings are often imprecise. Similar visual ratings are associated with a wide range of red, green, and blue brightness values. The

range of brightness values for different visual ratings overlap, thus minimum distances must be kept small enough that not all pixels in a specified rectangle are classified.

Table 3.1 Anova for visual data color ratings for 5 treatments, 2 rates on 3 trial dates.

	Trial 1 (6/26/95)				Trial 2 (7/10/95)				Trial 3 (7/18/95)			
SOURCE	df	ms	f	prob	df	ms	f	prob	df	ms	f	prob
Replication	2	0.533	1.0746	0.3623	2	2.800	4.5542	0.0251	2	0.900	1.6993	0.2109
treatment	4	3.117	6.2799	0.0024	4	4.217	6.8584	0.0015	4	2.450	4.6259	0.0096
rate	1	0.833	1.6791	0.2114	1	7.500	12.1988	0.0026	1	7.500	14.1608	0.0014
treatment x rate	4	0.417	0.8396	0.5260	4	0.917	1.4910	0.2466	4	0.417	0.7867	0.5490
Error	18	0.496			18	0.615			18	0.530		
Bartlett Test				0.000				0.000				0.000

Table 3.2 Anova for Computer assisted ratings for 5 treatments, 2 dates on 3 trials.

	Trial 1 (6/26/95)				Trial 2 (7/10/95)				Trial 3 (7/18/95)			
SOURCE	df	ms	f	prob	df	ms	f	prob	df	ms	f	prob
Replication	2	0.647	4.9005	0.0200	2	1.050	4.8818	0.0202	2	4.346	19.5612	0.0000
treatment	4	2.125	16.0997	0.0000	4	3.160	14.6884	0.0000	4	1.608	7.2374	0.0012
rate	1	2.526	19.1368	0.0004	1	2.855	13.2720	0.0019	1	1.637	7.3669	0.0142
treatment x rate	4	0.177	1.3378	0.2943	4	0.316	1.4682	0.2531	4	0.054	0.2446	0.9092
Error	18	0.132			18	0.215			18	0.222		
Bartlett Test				0.698				0.327				0.972

Table 3.3 Mean color rankings for visual ratings and computer assisted ratings.

		Trial 1 (6/26/95)				Trial 2 (7/10/95)				Trial 3 (7/18/95)			
		Visual		Computer		Visual		Computer		Visual		Computer	
Rate	Treatment	rating	Rank	rating	Rank	rating	Rank	rating	Rank	rating	Rank	rating	Rank
1	1	6.000	3	5.834	3	5.000	4	5.421	4	5.333	4	5.534	4
1	2	6.000	3	5.677	5	4.667	5	4.962	6	5.000	6	5.459	5
1	3	4.667	9	5.153	8	4.333	7	4.735	7	4.667	7	5.084	8
1	4	5.667	5	5.284	7	4.333	7	4.724	8	4.667	7	5.234	7
1	5	5.000	8	4.760	9	3.667	9	4.075	10	4.333	10	4.409	10
2	1	7.000	1	6.778	1	6.667	1	6.529	1	7.000	1	6.209	1
2	2	6.333	2	6.280	2	6.000	2	5.814	2	6.333	2	6.209	1
2	3	5.333	7	5.625	6	4.667	5	5.425	3	5.333	4	5.384	6
2	4	5.667	5	5.730	4	6.000	2	5.035	5	5.667	3	5.909	3
2	5	4.667	9	4.760	9	3.667	9	4.195	9	4.667	7	4.784	9
LSD		1.208		0.623		1.345		0.795		1.249		0.808	
CV		8.810		2.366		12.551		4.111		10.000		4.100	

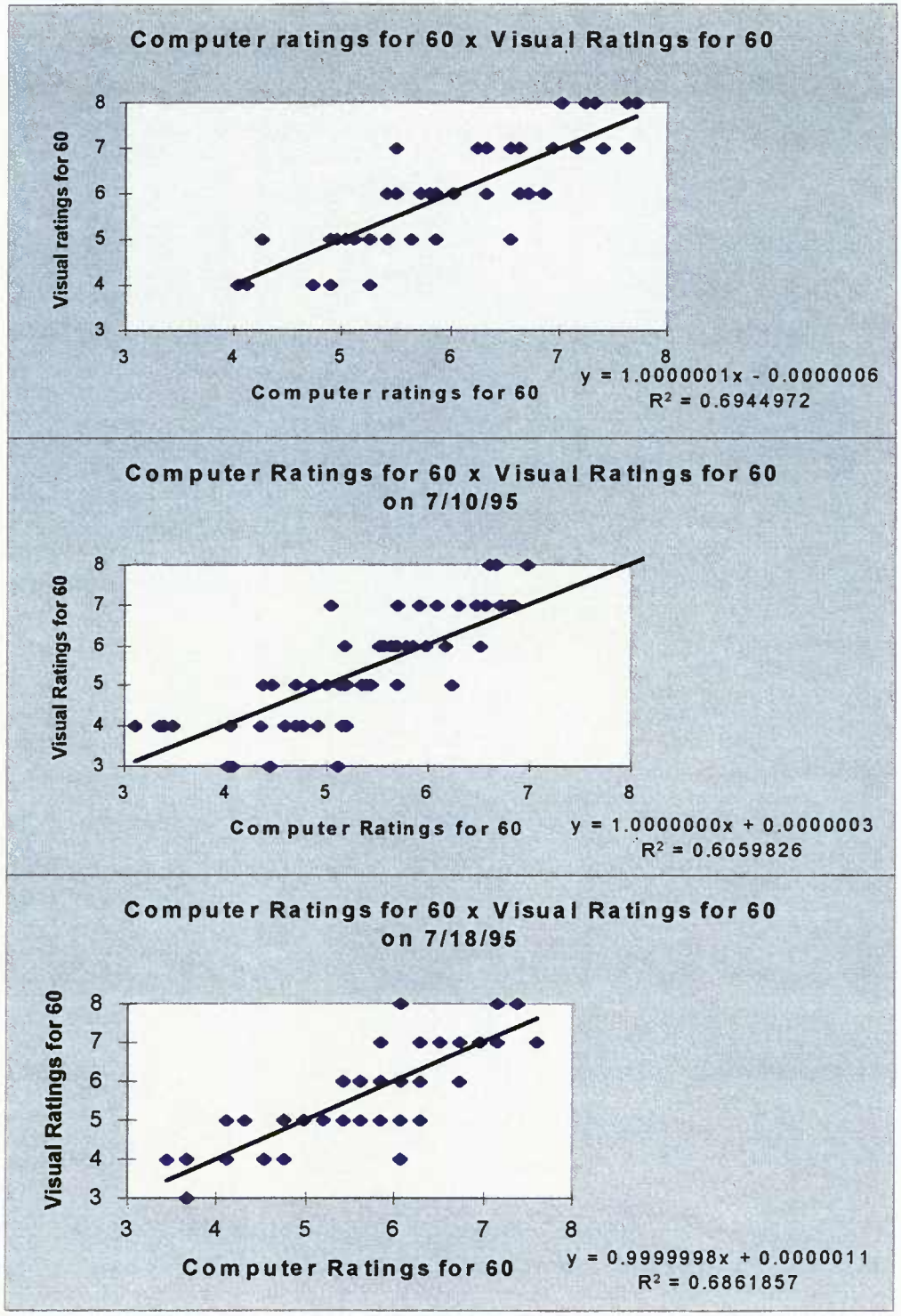

Figure 3.10 Comparison of computer ratings for 60 plots vs. visual ratings on 3 trial dates.

Conclusions

The tethered blimp or balloon systems can acquire digital images in a timely manner that is more cost efficient than conventional remotely sensed data. Although a wide variety of film types have been evaluated, standard color slide film has been chosen for routine use.

The supervised classification is dependent on prior knowledge of the evaluated plots. Visual rankings provide a range of possible values that are used to calibrate new computer-enhanced visual ratings.

Visual evaluations are unable to consistently measure and quantify small differences in color. This leads to less precise color quantification and generally limits color ratings to whole number intervals. The computer-enhanced visual ratings consistently had a higher probability of detecting differences between treatments. This increase in statistical precision was also accomplished without violating the assumptions for homogeneity of variance that visual ratings routinely violate. While more precise and objective than standard ratings, computer-enhanced visual ratings gave similar rankings.

This technique of digital analysis suggests it may be possible to provide supervised classification by predicting values for all plots given visual measurements of a few. Unsupervised classification may also be possible for all plots by giving a range of values. Supervised and unsupervised classifications are evaluated in the following chapter.

References Cited

Blinn, C.R., A. Lyos, and E.R. Buckner, 1988. Color aerial photography for assessing the need for fertilizers in Loblolly Pine plantations. Southern Journal of Applied Forestry 12:270-273.

Everitt, J.H., D.E. Escobar, R. Villarreal, M.A. Alaniz, and M.R. Davis,1993. Integration of airborne video, global positioning system and geographic information system technologies for detecting and mapping two woody legumes in rangelands. Weed Technology 7:981-987.

Harris, N.R., T.L. Righetti, and D.E. Johnson, 1995. Technical note: Monitoring rangelands and associated riparian zones with blimp borne cameras. Manuscript in Process. 11 pp.

Huete, A.R., R.D. Jackson, and D.F. Post, 1985. Spectral response of a plant canopy with different soil backgrounds. Remote Sensing of Environment 17:37-53.

Jackson, P.L., and G.G. Gaston, 1994. Digital enhancement as an aid to detecting patterns of vegetation stress using medium-scale aerial photography. International Journal of Remote Sensing. 15:1009-1018.

Liu, J.G. and J. McM. Moore, 1990. Hue image RGB colour composition. A simple technique to suppress shadow and enhance spectral signature. International Journal of Remote Sensing. 11(8): 1521-1530.

Malthus, T.J. and A.C. Madeira, 1993. High resolution spectroradiometry: Spectral reflectance of field bean leaves infected by *Botrytis fabae.* Remote Sensing of Environment 45:107-116.

Penuelas, J., J.A. Gamon, K.L. Griffin, and C.B. Field, 1993. Assessing community type, plant biomass, pigment composition, and photosynthetic efficiency of aquatic vegetation from spectral reflectance. Remote Sensing of Environment 46:110-118.

Penuelas, J., J.A. Gamon, A.L. Fredeen, J. Merino, and C.B. Field, 1994. Reflectance indices associated with physiological changes in nitrogen- and water-limited sunflower leaves. Remote Sensing of Environment 48:135-146.

Ribeiro, O.K., C.G. Crabtree, and E.B. Henrickson, 1994. Possible role of multispectral imagery for the detection of stress vectors in apple replant situations. Acta-Horticulturae 363:169-174.

Toler,R.W., B.D. Smith, and J.C. Harlan, 1981. From Hand-Held Cameras to Remote Sensing Techniques. Plant Disease 65:25-31.

Wildman, W.E., R.T. Nagauka, and L.A. Lider, 1983. Monitoring spread of Grape Phylloxera by color infrared aerial photography and ground investigation. American Journal of Viticulture 34:83-94.

Wildman, W.E., W. Bowers, and L.T. Bettiga, L.T. 1992. Aerial photography in vineyard pest, soil and water management. Grape Pest Management. Ag Sciences Publications, Berkely Press pp. 30-35.

Yoder, B.J. and R.E. Pettigrew-Crosby, 1995. Predicting nitrogen and chlorophyll content and concentrations from reflectance spectra (400-2500 nm) at leaf and canopy scales. Remote Sensing of Environment 53:199-211.

Chapter 4

SUPERVISED AND UNSUPERVISED CLASSIFICATION OF TURFGRASS BY SPECTRAL PATTERN RECOGNITION AND REGRESSION

William Friedkin

To be submitted to *Journal for the American Society of Horticultural Science,* with Richard Matteson, T.L. Righetti, and Tom Cook as co-authors.

Abstract

CLASSIFICATION BY SPECTRAL PATTERN RECOGNITION AND REGRESSION IN TURFGRASS

William Friedkin

Most conventional approaches to rating turf color employ a visual subjective rating. Original visual ratings of turf plots can be used to calibrate remote images. Linear relationships between visual ratings and data from histograms of the red, green, and blue bands on the same plots have been used to predict new computer enhanced ratings.

In this investigation, supervised classifications were evaluated. Predictions for 60 turf plots were made from visual evaluations of a series of 6, 12, and 18 random and color range selected reference plots. Unsupervised classification was achieved by applying principal components transformation to the histogram data and selecting the first principal component as a rating value. These values are then scaled to fit within the traditional 1-9 turf rating system by supplying minimum and maximum values.

Eighteen color range selected plots were required to insure accurate predictions. Further improvement occurred if predictions from the 18 color range selected reference plots were rank adjusted to the minimum and maximum values for the reference set. The 18 plot supervised classifications did not violate assumptions for ANOVA where visual ratings did. Statistical significance was generally greater for the supervised classification than the visual data.

Unsupervised classifications predicted values that were consistent with the original visual ratings in two of three trials. Although unsupervised classifications and visual ratings of plots were weakly related in one trial, the relative rankings of unsupervised classification and visually rated means is very similar for all three trials. Differences in predicted values were more statistically significant than visual ratings.

Introduction

Visually rating turf plots is tedious. Rating hundreds of plots requires a standardization that cannot be maintained from beginning to end. Physical limitations of the evaluator usually result in whole number rankings that cause violations of assumptions for homogeneity of variance in ANOVA (Chapter 3). An accurate and consistent evaluation procedure that produces statistically separable differences between experimental treatments is desired.

Remote sensing has been used as a crop management tool for many years (Toler et al., 1981; Wildman et al., 1983; Wildman et al., 1992; Everitt et al., 1993). Digital image analysis traditionally has made use of visual interpretation of color-infrared aerial photos to detect differences in biomass, color tone or soil color (Wildman et al., 1992). Color photography from tethered blimp systems has been used to produce computer enhanced visual ratings (Chapter 3). These ratings have similar relative rankings, but are more statistically precise than the original visual ratings.

Most supervised classification schemes use mid range values of red, green, or blue bands. However, other positions on a histogram contain useful information. Various transformations or indices calculated from raw data are also valuable (Penuelas et al., 1994). However, traditional indices are also dependent on mid range values within the respective spectral bands. Indices can be calculated using values from any position on a histogram. With multiple points along each of the three color planes (red, green and blue), it was possible to have multiple user defined indices within and between the color bands. With multiple values extracted from the original histograms and various user specified ratios and indices calculated from those values, between 60 and 100 color variables (many of which are more strongly related to color ratings than red, green, or blue means) were used to describe each plot (Chapter 3). Linear regression equations between these color variables and visual plot ratings are calculated. The desired equation (with the highest R^2) was used to produce a predicted or classification rating for all the

plots within the trial. Predicted values have a higher probability of consistently detecting differences between treatments than original visual ratings. This increase in statistical precision was accomplished without violating the assumptions for homogeneity of variance.

Computer enhance visual ratings use all of the evaluated plots to calculate regression equations that are used to produce new ratings for each plot (Chapter 3). The utility of the procedure could be improved if accurate ratings could be made using a portion of the plots to develop regression equations to rate an entire experiment.

In this presentation, we evaluate the success of supervised classifications using either 6, 12, or 18 training sites to predict values for a 60 plot experiment. We also attempted unsupervised classifications that could be made without using training sites.

For supervised classification, we allow the user to find the best fit linear relationship between the visual rating from sample turf plots and the spectral response pattern as defined by the red, green, and blue histograms and associated indices. Ratings for all turf plots are made by applying the selected regression equation. Our hypothesis is that the predicted plot color ratings would be more accurate and statistically robust than rating all study plots visually.

For unsupervised classification, a principal components analysis was used to minimize redundancy between the red, green, and blue histogram values. The first principal component accounts for the highest amount of variance for the whole dataset. The first principal component is then rescaled to a range of classes that defines an objective color rating for high and low ratings within the image. Our hypothesis is that by applying principal components analysis to the spectral data and scaling their results, we can have a more accurate and statistically robust classification than by visual rating.

Materials and Methods

Blimp, Cameras, Film and Development

We have used a gimbaled camera box suspended from a 5.1 m^3 helium-filled blimp to carry a Canon EOS 35mm camera loaded with Fuji Velvia film, and fitted with a Sigma 28 mm (f/1.8) lens (Chapter 3). Focus is manually set to infinity. A small propeller is mounted on the box for manual orientation. Radio-controlled servos, transmitters, and receivers are used to control the propeller for orientation and for shutter operation. The blimp was flown between 61 and 122 m above the turf plots, located at Oregon State University's Lewis- Brown Farm in Corvallis, Oregon. Slides of the turf plots were locally developed using the standard E4 process.

Plot Layout and Design

The study described below was designed to rate fertilizer efficiency/response through visual color ratings on ryegrass turf. Three dates (6/26/95, 7/10/95 and 7/18/95) are treated as separate trials for comparison of visual ratings, computer enhanced visual ratings (Chapter 3), supervised, and unsupervised classification evaluations. All plots were visually rated and photographed on the same day.

The study area is 12.8 m long by 12.2 m wide. The turf trial consists of sixty - 1.2 m by 1.5 m plots. They are arranged in 6 rows each - 10 plots long. Each plot is surrounded by a 7.6 cm wide herbicide strip. The turf trial consists of three replications in a complete random block design. There are 20 treatments; 9 fertilizer sources at 2 rates (.0048 and .0096 kg • m^2 N), one fertilizer source at a single rate and the control (Chapter 3).

Digital Processing

Full color photographs were processed into slides. The 35mm slides in these evaluations were scanned with a Polaroid Sprintscan into 24-bit color images in .bmp (bitmap) format..

We have decided on an approximately 650 x 650 pixel spatial resolution as a compromise between increasing resolution and manageable storage and processing size. Although up to a 4000 x 6000 pixel resolution is possible, we have found few advantages to using greater resolution that requires longer processing times with increasing storage problems. Steps in digital processing are as follows:

1) A scaled drawing of all treatment plots is oriented north and south and plot corners are located as control points. The .dxf drawing (drawing exchange file) has two layers. The first layer is the outline of the plots. A second layer consists of horizontal lines used for plot selection. The plots are ordered west to east along the row, consecutively north to south between rows. The order in which these lines are drawn is associated with the sequential order of the previously obtained visual ratings. Visual ratings are on a scale of 1 to 9 and are entered into a tab delimited .txt file with each entry in a separate, numbered row.
2) After digitization, 24-bit images are brought into Easy Image and separated three 8-bit planes (red, green and blue). The operator chooses one of the bands (usually the green) and, using a thresholding routine, creates a mask to remove either shadows or bare spots from the photograph.
3) The three thresholded bands are then rectified to the scaled drawing. The size of the plot borders in the drawing (15 cm) are large enough that rectification need not be perfect. In this example, pixel size is 23 cm^2 .
4) The software calculates a histogram for each of the three color bands for each plot as defined by the grid drawing. Frequency of occurrence (f) is plotted along the

vertical axis with individual measurements of pixel intensity between 0 and 255 along the horizontal axis (Chapter 3). The median pixel value, its corresponding y value and 8 other points that characterize a smoothed histogram are saved to a file for the red, green, and blue bands for each designated plot. Several indices and ratios are calculated using the values from the respective multiple points within the generated histograms.

There are two ways to predict class membership from the histogram. There is a supervised classification in which an unknown pixel value is predicted by its relationship to a spectral and/or statistical pattern derived from a training site data set. And there is the unsupervised classification, in which the unknown pixel value assignment is based on a statistical and/or spectral pattern alone. Our approach in this presentation is to extract pixel information from 24-bit images and quantify those values for both types of classification.

Supervised Classification

Training sites are selected by entering a horizontal line on the plot diagram within the respective plots. The number of training sites used in the supervised classification is varied to determine the optimal, minimum number of sites required to accurately assess the color evaluation procedure. The actual number of plots to be referenced as training sites are arbitrarily set at 6, 12, and 18 plots, respectively, from a set of 60 plots within the trial site. We used both a stratified random sampling and a range selection to choose the reference plots to predict values for the entire experiment. For stratified random sampling, we randomly selected 1, 2, or 3 plots from each row. For the color range selection, 1 to 3 representative plots with low and high visual valuations were selected along with 4, 8, or 12 additional randomly selected plots irrespective of block and row boundaries. Seven different sets of training sites were evaluated for each sample

number size (i.e. 7 /6 plot training sites, 7 /12 plot training sites and 7 /18 plot training sites) for each selection procedure.

With 54 values extracted from each of the original histograms (9 points, each with an X and Y value for each band) and various user defined ratios and indices calculated from those values, we generate 69 color variables describing each plot. Linear regression equations that define the relationship between the color variables for each of the sampled plots and the respective visual ratings are calculated and presented in order of decreasing R^2 values. The regression for the highest R^2 is applied to histograms from every plot to produce a predicted rating or classification for all the plots within the trial.

Since visual turf grass evaluations rank color on a scale from 1 to 9 and our ratings fell between 3 and 8, the predicted values were rescaled to that range of classes. The range selection by 3 and 8 represent the minimum and maximum values in the reference plots. The same extremes were also used to rescale stratified random reference plots even though values of 3 and 8 did not always occur.

We assumed that a regression using all plots (full regression) for training sites and recalculation of new values for each plot was ideal. Regressions between 21 supervised classification predictions (7 sets each for 6, 12, and 18 reference plot sample sizes) and the full regression predictions were used to quantify the success of the three sample sizes for the stratified random and by range selections. Visual color and digital classification ratings were analyzed by ANOVA with mean separation by LSD. Since design was not a complete factorial, it was evaluated both as a 20 treatment trial, and as a factorial experiment with 5 formulations at two rates (treatments 1 - 5 and treatments 7 - 11). Microsoft Excel 6.0 software was used for the regression analysis and rescaling transformations. Systat for Windows was used for the two factor randomized block ANOVA.

Unsupervised Classification

Histograms were selected for all 60 plots within the trial. Principal components analysis was applied to the 27 color variables (intercept Y values were not included), corresponding vegetative indices, and mid-range ratios. The first principal component values were rescaled to fit the 3 to 8 range as previously described.

Regression between unsupervised predictions and the full regressions were evaluated and an ANOVA of the predicted values was conducted as described above. Systat for Windows 6.0 was used for principal components analysis.

Results and Discussion

Computer-assisted ratings result from using all plots as training sites. They have a higher probability of detecting differences between treatments than visual ratings without violating the assumptions of homogeneity of variance (Friedkin, W. et al., 1996). ANOVAs for computer-assisted ratings or full regression predictions produce the lowest MSE among all prediction procedures (Fig. 4.1). Because of this statistical precision, computer-assisted ratings are used as a standard by which to measure accuracy for supervised and unsupervised classifications.

. The MSE for selected sampling in supervised classification is lower than random sampling values for all three trials in 12 sample and 18 sample regression predictions. The MSE for the 18 sample regression predictions is lower than visual ratings in two of three trials and approximately equal to the third. Using 18 color range selected samples as testing sites is superior to other sampling schemes.

The correlation of 6, 12, and 18 random sample predictions with computer-assisted ratings varies with the difference in the number of samples (Fig. 4.2). With increasing number of samples, the average R^2 for all 7 replicate sampling increases. However, even eighteen sample regression predictions are not consistent in their ability to correlate with computer-assisted ratings. Replicate three (18c), for Trial 2 produces values weakly

related to computer assisted ratings as does 18b, 18d, 18f and 18e for Trial 3. Predictions from 18 selected samples are consistent with computer-assisted ratings for all (Fig. 4.3). All predictions have an R^2 of 0.80 or higher between replicates. Six-sample and 12-sample replicates fail to consistently correlate with computer-assisted ratings. These results are compatible with mean square error ratings as demonstrated above, and further support using a minimum of 18 range selected samples.

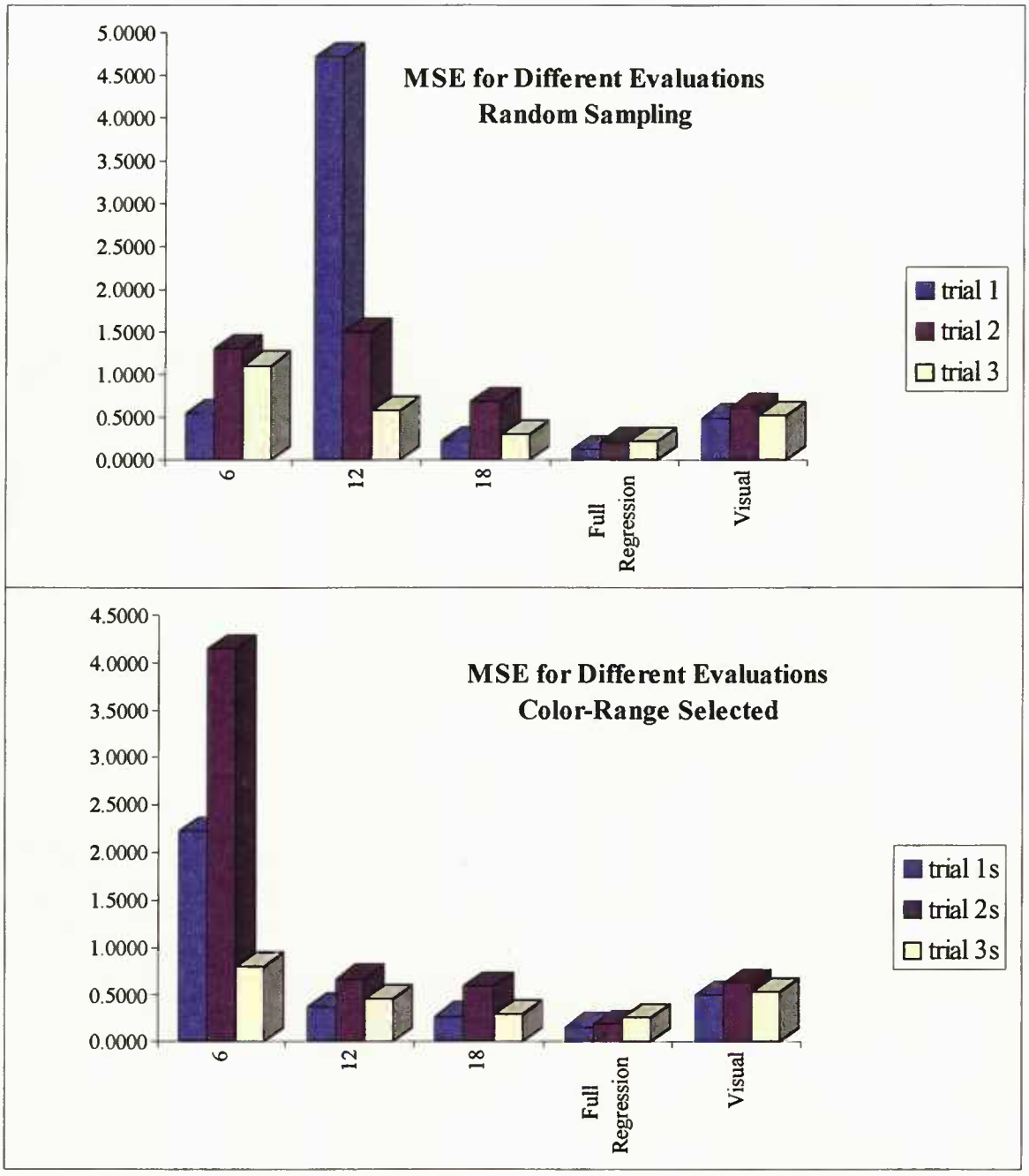

Figure 4.1 The mean square error from ANOVA evaluations of stratified random sampling from evaluations from selected training sites.

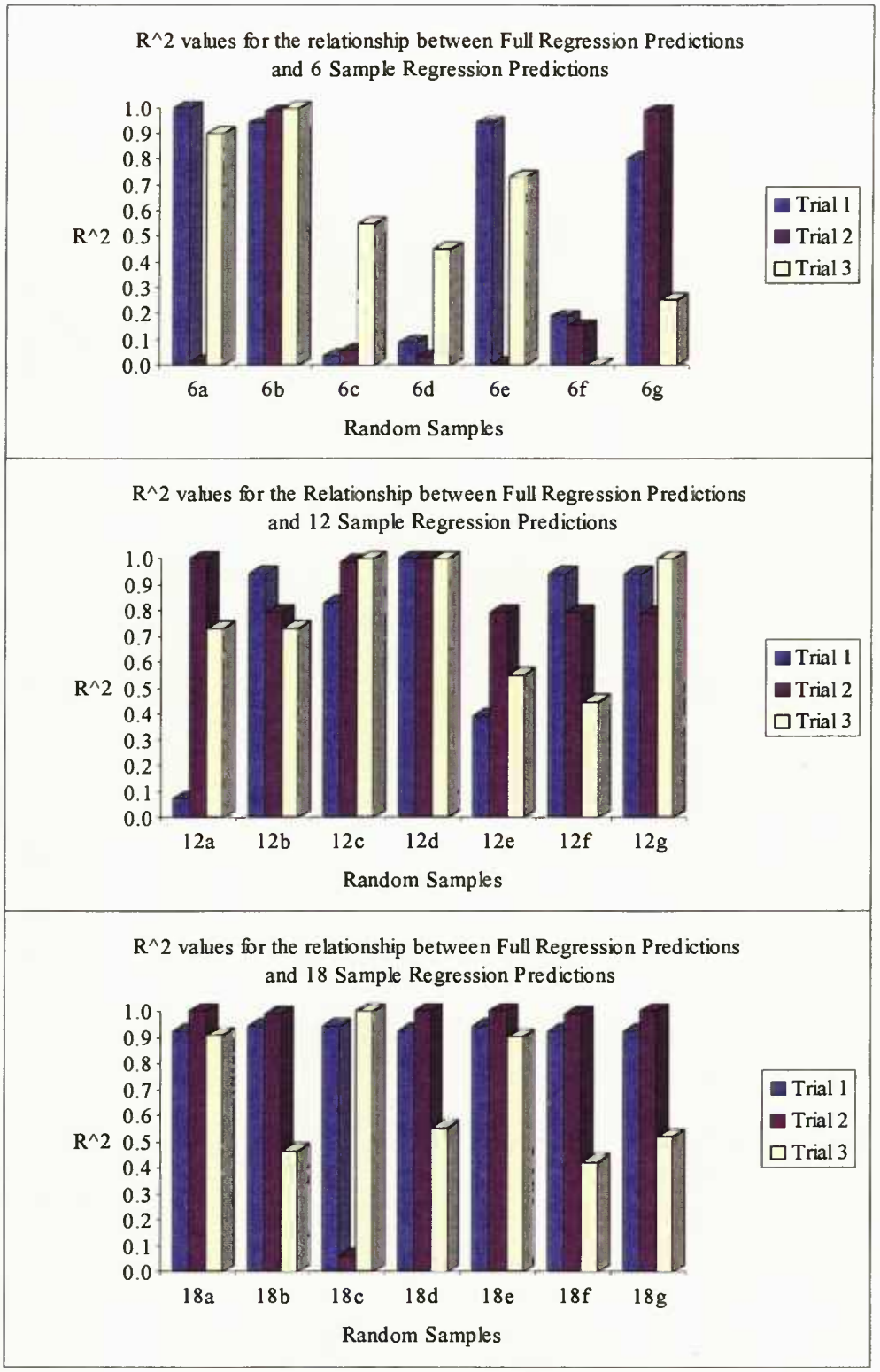

Figure 4.2 The relationships between predictions from computer-assisted ratings and the predictions by regression from 6, 12, or 18 stratified random samples

When predicting by regression, the slope of the regression equation can produce prediction errors. Minimum and maximum predicted values are often exaggerated (Fig. 4.4). These errors decrease as the number of samples increase, but some variability is apparent even in 18 color range selected reference sample regressions. Mean and median values also change but are less variable than the extremes. By applying a scaling procedure to the selected sample regression predictions and scaling all values to be within the range of the calibration set, minimum and maximum values remain similar for all predictions (Fig. 4.5). Distributions are 'normalized' about the mean in all replicates and standard deviations are similar.

The full regression predictions produced significant differences for formula, rate, and replication (block) while formula rate interactions were not significant (Fig. 4.4). Six-sample predictions were not able to detect significant differences in all replicates. Twelve-sample predictions were unable to detect differences in rate effect in replicate 7 (n12g). Eighteen-sample predictions were consistent in detecting significant rate and treatment effects and in their ability to detect possible treatment differences in all replicates. In no instance was there any significant effect of rate on formulation (formula x rate interaction). Rate is independent of formulation. Unlike visual ratings, significant differences in replication were always detected in either 12 or 18 sample reference plots. The detection of block effects increases the ability to detect treatment differences.

The unsupervised classification detected significant differences in replication, treatment and rate in all three trials (Tables 4.1 and 4.2). The mean square error is lower for unsupervised classification than for visual MSE in all three trials. A comparison of the coefficients of variation indicates there are 1.7, 3.1, and 1.2 times more variability among plots within treatments for visual ratings than in unsupervised ratings for Trials 1, 2, and 3 respectively. There is always a higher level of significance for treatment differences in the unsupervised classifications and a higher level of significance for rate in 2 of 3 trials.

Although the relative ranking of means is very similar to original visual rankings for all trials for unsupervised classification, visual color ratings are dissimilar from unsupervised ratings in Trial 2 and unsupervised ratings were not as strongly related to the full regression predictions. R^2 values between full regressions and supervised classifications are .96, .74, and .95 for Trials 1, 2, and 3, respectively.

The failure of unsupervised classification to strongly relate to full regression or to visual ratings may be due to the spectral characteristic of the image for Trial 2 (Fig. 4.7). The Trial 2 color band characterizations for the whole image have no distinct mid-range value in the red band, relatively high minimum brightness values in all three bands and distinct or separable color brightness values for each band. The principal component transformation effectively separated the color bands while eliminating the redundancy. The 2^{nd} principal component had a higher R^2 for the relationship with the visual ratings than the 1^{st} principal component (data not shown). Trial 3 had a very narrow distribution of brightness values on the low end of the brightness scale and skewed distributions. Low image contrast or narrow distributions of brightness values (DN or digital number values) may increase the difficulty in discrimination by lag point definition on the frequency distribution. A wide the range of DN values in all bands and low albedo (relatively high frequencies and low minimum brightness values) may provide for better utilization of principal component procedures.

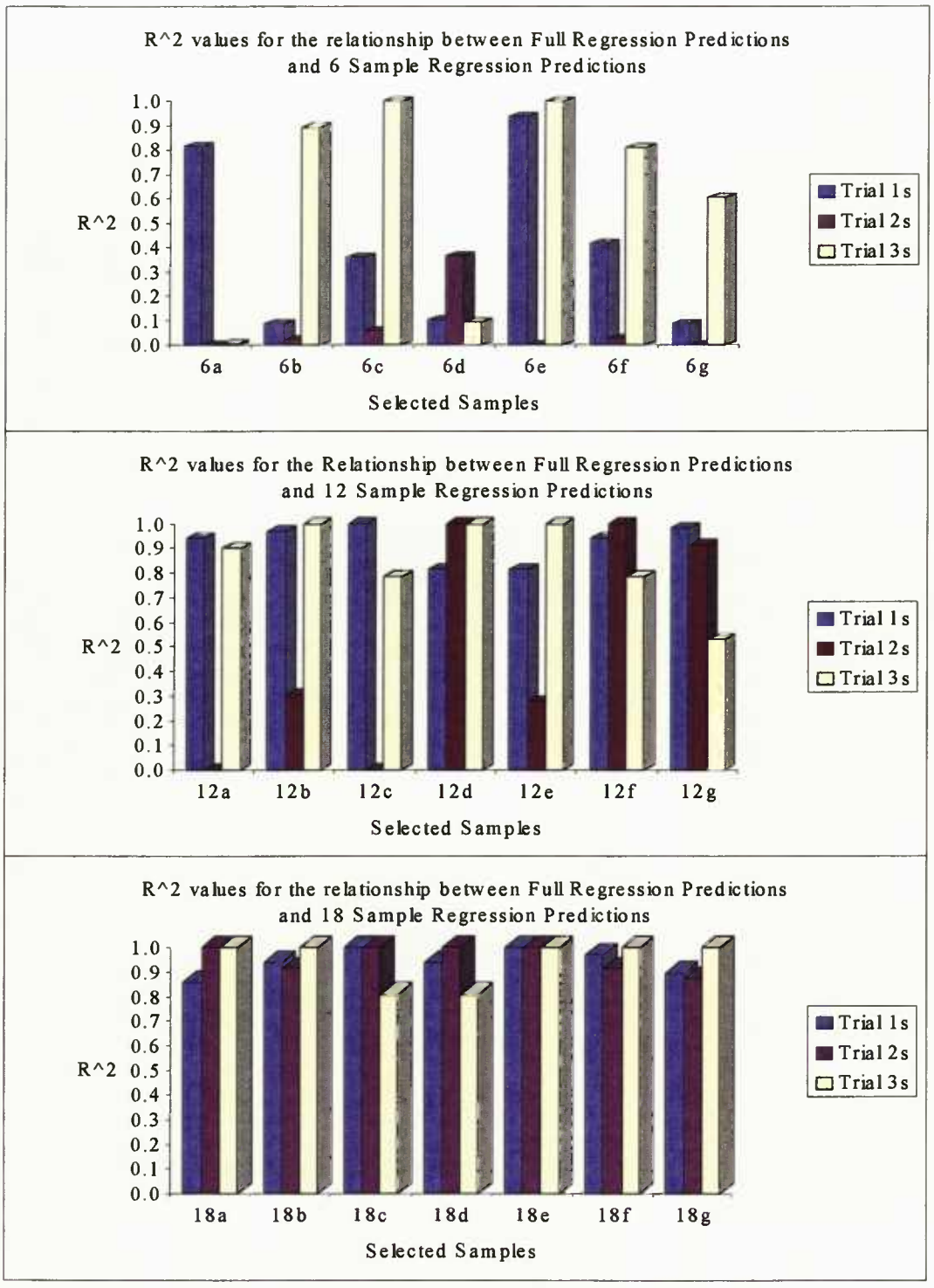

Figure 4.3 The relationships between predictions from computer-assisted ratings and the predictions by regression from 6, 12, or 18 selected samples and their respective spectral signatures

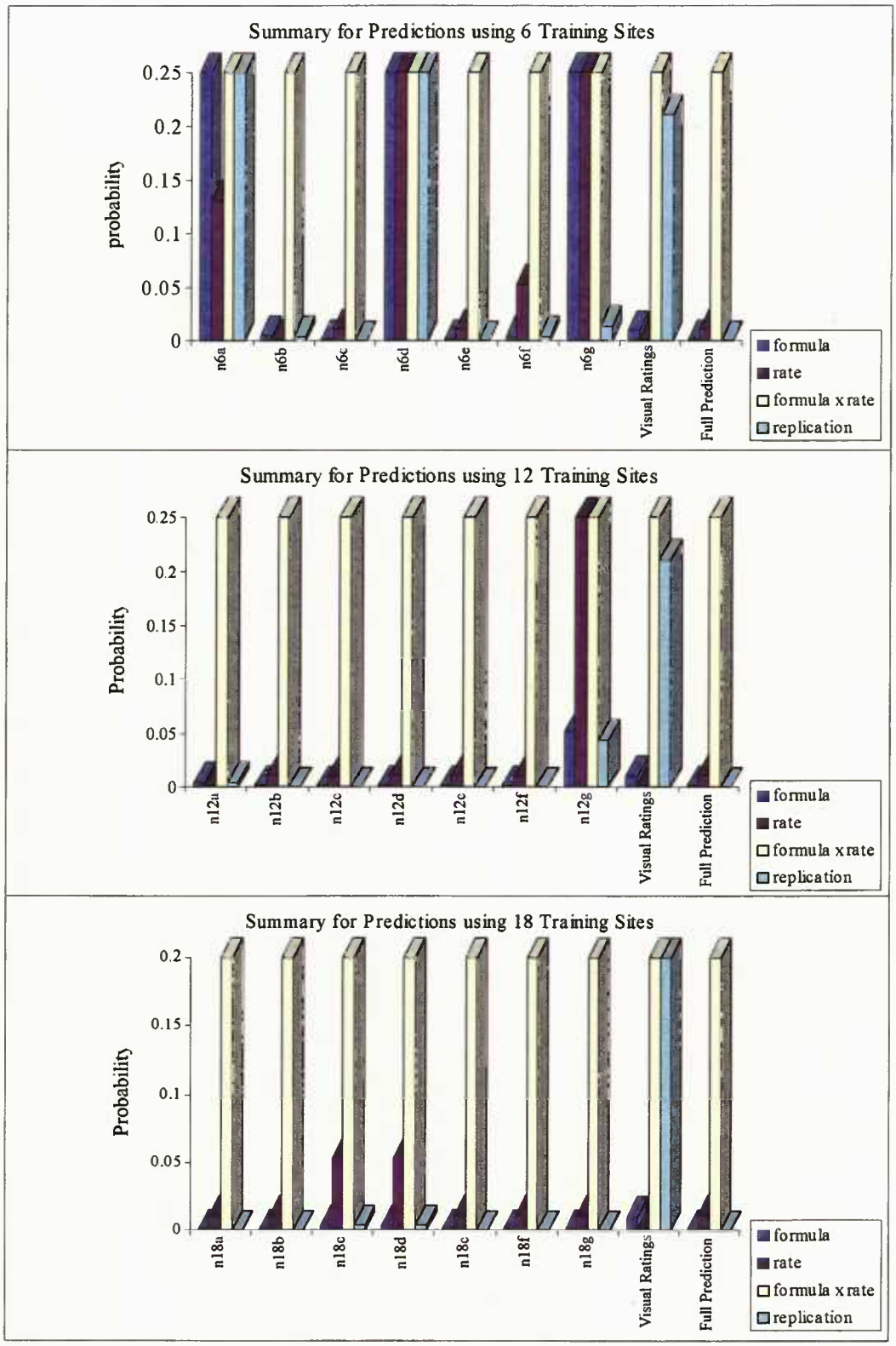

Figure 4.4 The significance of predictions made by 6, 12, and 18 training sites for supervised classification.

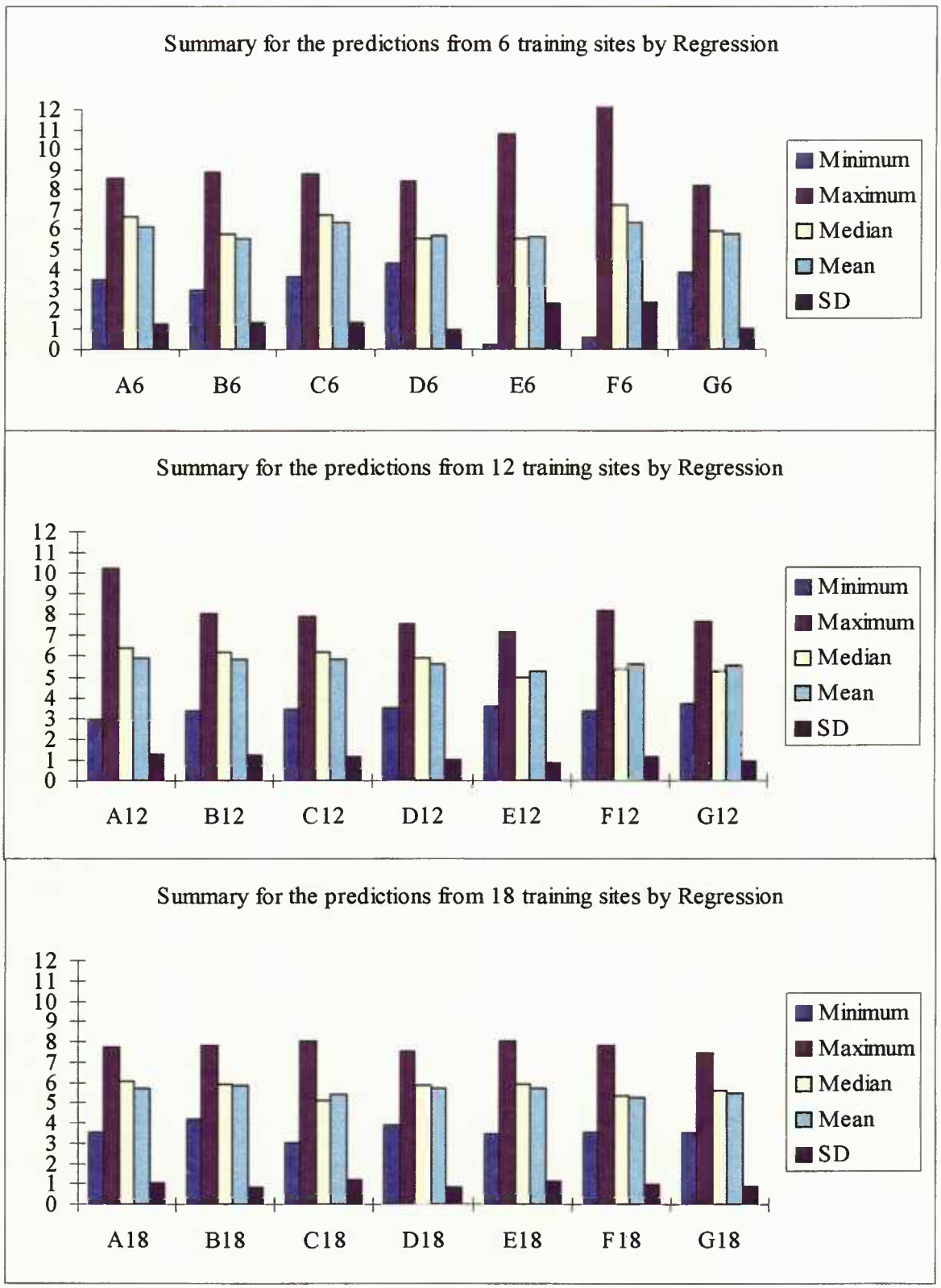

Figure 4.5 The summary of minimum, maximum, median, mean, and standard deviations for supervised classification from color range selected reference plots.

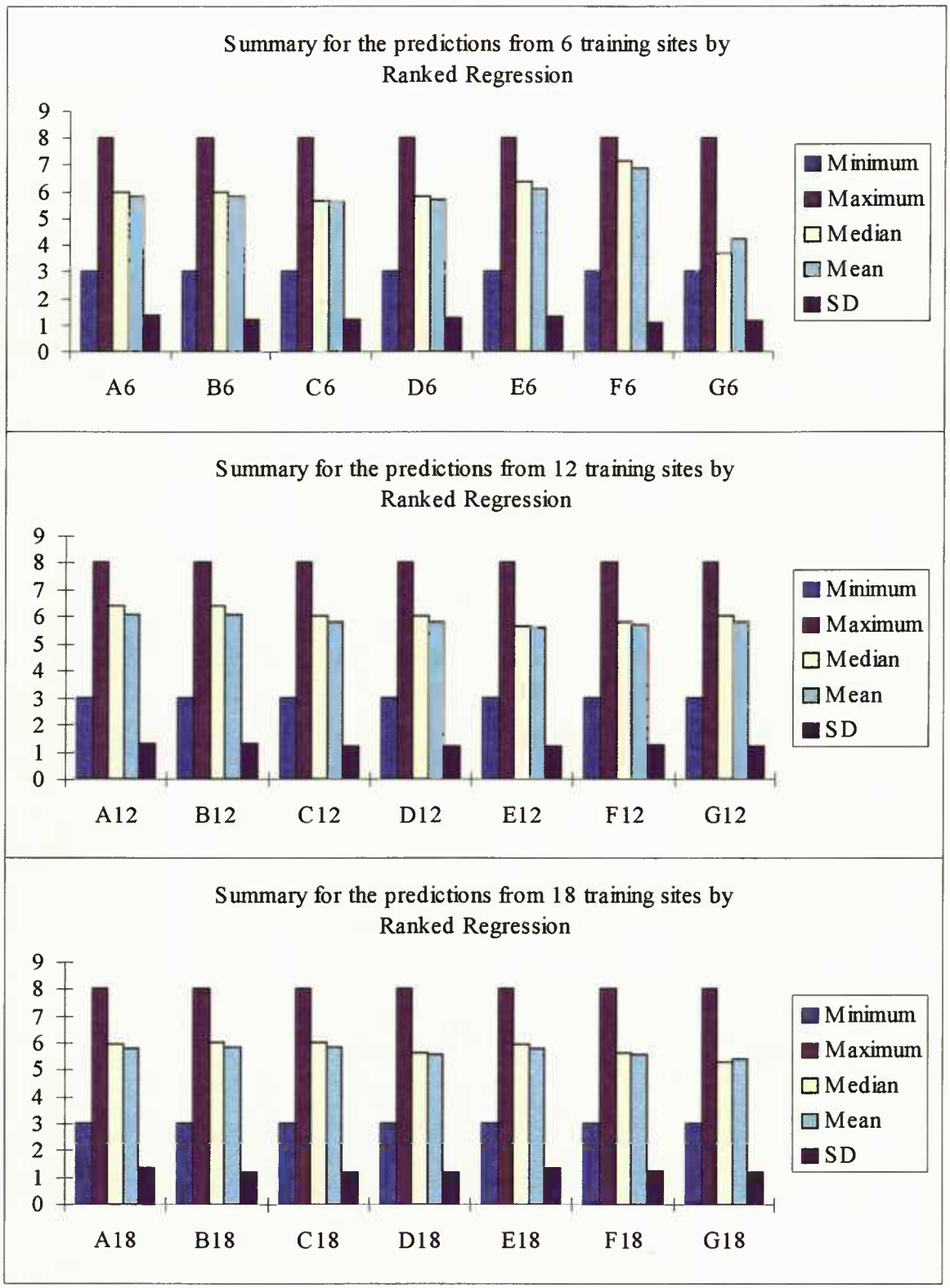

Figure 4.6 The summary of minimum, maximum, median, mean, and standard deviations for supervised classification from ranked color range selected reference plots.

Table 4.1 Anova for visual data color ratings for 5 treatments, 2 rates on 3 trial dates.

	Trial 1 (6/26/95)				Trial 2 (7/10/95)				Trial 3 (7/18/95)			
SOURCE	df	ms	f	prob	df	ms	f	prob	df	ms	f	prob
Replication	2	0.533	1.0746	0.3623	2	2.800	4.5542	0.0251	2	0.900	1.6993	0.2109
treatment	4	3.117	6.2799	0.0024	4	4.217	6.8584	0.0015	4	2.450	4.6259	0.0096
rate	1	0.833	1.6791	0.2114	1	7.500	12.1988	0.0026	1	7.500	14.1608	0.0014
treatment x rate	4	0.417	0.8396	0.5260	4	0.917	1.4910	0.2466	4	0.417	0.7867	0.5490
Error	18	0.496			18	0.615			18	0.530		

Table 4.2 Anova for unsupervised classification ratings for 5 treatments, 2 rates on 3 dates.

	Trial 1 (6/26/95)				Trial 2 (7/10/95)				Trial 3 (7/18/95)			
SOURCE	df	ms	f	prob	df	ms	f	prob	df	ms	f	prob
Replication	2	1.138	4.2790	0.0302	2	5.182	25.1774	0.0000	2	4.894	10.5246	0.0009
treatment	4	4.700	17.6684	0.0000	4	3.475	16.8856	0.0000	4	2.792	6.0038	0.0030
rate	1	3.533	13.2817	0.0019	1	3.037	14.7581	0.0012	1	4.175	8.9799	0.0077
treatment x rate	4	0.275	1.0326	0.4175	4	0.236	1.1488	0.3657	4	0.198	0.4250	0.7886
Error	18	0.266			18	0.206			18	0.465		

Table 4.3 Mean color rankings for visual ratings and unsupervised classification.

		Trial 1 (6/26/95)				Trial 2 (7/10/95)				Trial 3 (7/18/95)			
		Visual		Computer		Visual		Computer		Visual		Computer	
rate	treatment	rating	Rank	rating	Rank	rating	Rank	rating	Rank	rating	Rank	rating	Rank
1	1	6.000	3	5.604	3	5.000	4	5.844	3	5.333	4	5.627	4
1	2	6.000	3	5.123	6	4.667	5	5.033	6	5.000	6	5.538	6
1	3	4.667	9	4.680	8	4.333	7	4.962	7	4.667	7	5.020	8
1	4	5.667	5	4.783	7	4.333	7	4.740	8	4.667	7	5.285	7
1	5	5.000	8	3.761	10	3.667	9	3.986	10	4.333	10	4.374	10
2	1	7.000	1	6.640	1	6.667	1	6.389	1	7.000	1	6.703	1
2	2	6.333	2	6.172	2	6.000	2	6.334	2	6.333	2	6.627	2
2	3	5.333	7	5.212	5	4.667	5	5.565	4	5.333	4	5.563	5
2	4	5.667	5	5.576	4	6.000	2	5.236	5	5.667	3	6.070	3
2	5	4.667	9	3.782	9	3.667	9	4.223	9	4.667	7	4.613	9
LSD		1.208		0.885		1.345		0.779		1.249		1.169	
CV		8.81		5.185		12.55		4.043		10		8.394	

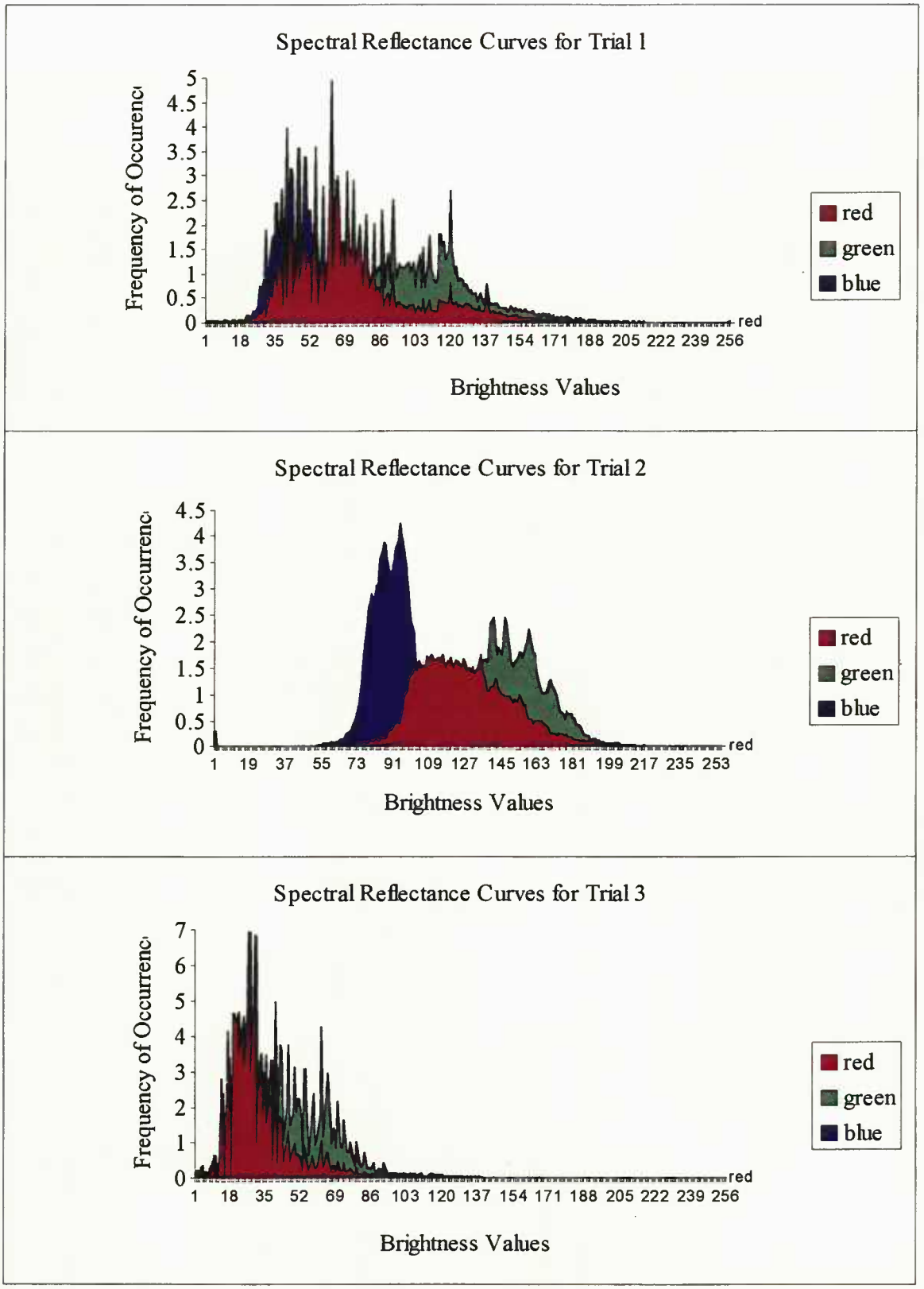

Figure 4.7 Spectral reflectance curves for each of three trials.

Conclusions

As the number of training sites increase, statistical precision and prediction accuracy increase. Predictions made by regression from 18 training sites consistently had a higher probability of detecting differences between treatments than visual ratings alone. This increase in statistical precision is accomplished without violating the assumptions for homogeneity of variance. Color range selection of training sites increases precision.

Minimum and maximum predicted values are sometimes exaggerated in regression predictions. By applying a scaling procedure such that all values will be within the range of the calibration set, those errors are eliminated. Using 18 color range selected calibration sets with scaled prediction values produces a precise and objective classification whose results are as nearly accurate as the computer assisted ratings and are more statistically robust than visual ratings.

If resources are available, the choice for classification in order of precision would proceed by order of computer-assisted classification, supervised classification, unsupervised classification, and then visual rating. Supervised classifications are timely, economic and more statistically robust than visual rating alone.

Unsupervised predictions are especially attractive because no calibration plots are required. Minimum and maximum values are all that are required to scale principal component analysis.

Unsupervised predictions may be possible but procedures need to be improved to develop workable systems that are broadly applicable to different image characteristics. The strong relationship between unsupervised predictions and computer assisted ratings in two of the three trials is encouraging. Even in the trial that was less successful, the relative rankings of treatment means is very similar to the original visual rankings

References Cited

Baker, J.R., S.A.Briggs, V. Gordon, A.R. Jones, J.J. Settle, J.R.G. Townshend, and B.K. Wyatt, 1991. Advances in classification for land cover mapping using SPOT HRV imagery. Int. J. of Remote Sensing 12: 1071-1085.

Botkin, D.B., J.E. Estes, R.M. MacDonald, and M.V. Wilson, 1984. Studying the earth's vegetation from space. Bioscience 34: 508-514.

Cetin, H. and D.W. Levandowski, 1991. Interactive classification and mapping of multi-dimensional remotely sensed data using n-dimensional probability density functions (nPDF). Photogrammetric Engineering and Remote Sensing 57: 1579-1587.

Dobson, J.E, 1993. Commentary: A Conceptual Framework of integrating Remote Sensing. Photogrammetric Engineering and Remote Sensing 59:1491-96.

Estes, J.E. 1992. Remote Sensing and GIS Integration : Research needs status and trends. ITC J. 1992(1): 2-10.

Fisher, P.F. and S. Pathirana, 1990. The evaluation of fuzzy membership of land cover classes in sub zones. Remote Sensing of Environ. 34: 121-132.

Franklin, S.E. and B.A.Wilson, 1992. A three-stage classifier for remote sensing of mountain environments. Photogrammetric Engineering and Remote Sensing 58: 449-454.

Friedkin, W., T.L. Righetti, and T. Cook, 1996. Digital analysis of remotely sensed images for evaluating color in turfgrass. Manuscript in process. 19 pgs.

Gong, P. and P. Howarth. 1992. Frequency based contextual classification and gray level vector reduction for land use identification. Photogrammetric Engineering and Remote Sensing 58: 423-27.

Harding, P.J. and C.N. Thomson. 1992. Fast nearest neighbor classification methods for multispectral images. Professional Photographer 44: 191-201.

Jahne, B, 1993. Digital image processing. Springer-Verlag, New York.

Jain, A.K, 1989. Fundamentals of digital image processing. Prentice Hall, New Jersey.

Jensen, J.R. 1996. Introductory digital image processing. Prentice Hall, New Jersey.

Jensen, J.R. and D.L. Toll, 1982. Detecting residential land use development at the urban fringe. Photogrammetric Engineering and Remote Sensing 48: 629-643.

Labovitz, M.L. and E.J. Masvoka. 1984. The influence of auotcorrelation in signature extraction - An example from a geobotanical inventory of Cotterbasin, Montana. International Journal of Remote Sensing 5: 315-332.

Mahar, H. and M.S. Afifi, 1995. Linear and correlation analysis for computerized identification of categories in Landsat images. Int. J. of Remote Sensing 16: 2277-2284.

Meyer, M. and L. Werth 1990. Satellite data: Management panacea or potential problem? Journal of Forestry 88(9): 10-13.

Schalkoff, R. 1992. Pattern recognition: Statistical, structural and neural approaches. New York: John Wiley, 364 pp.

Swain, D.H. and S.M. Davis. 1978. Remote Sensing: The quantitative approach. New York: McGraw Hill, 166-174.

Wang, F. 1990a. Fuzzy supervised classification of remote sensing images. IEEE Transactions on Geoscience and Remote Sensing 28: 194-201.

Wang, F. 1990b. Improving remote sensing image analysis through fuzzy information representation. Photogrammetric Engineering and Remote Sensing. 56:1163-1169.

Wang, F. 1991c. Integrating GIS's and remote sensing image analysis systems by unifying knowledge representation schemes. IEEE Transactions on Geoscience and Remote Sensing. 29: 656-664.

Zahn, C.T. 1971. Graph-theoretical methods for detecting and describing gestalt clusters. IEEE Transactions on Computers C-20(1): 68-86.

CONCLUSIONS

The tethered blimp or balloon systems can acquire digital images in a timely manner that is more cost efficient than conventional remotely sensed data. Low altitude photography provides high spatial resolution. Spatial resolution is approximately 2.5 cm/pixel for the tethered blimp versus 10 meters/pixel for SPOT panchromatic for all color bands within the color image.

We have used histogram characterization as a means for spectral/spatial pattern recognition. Frequency of occurrence is plotted along the vertical axis with individual measurements of brightness along the horizontal axis. A sequential pattern of recognition points is defined for each color band histogram. Lag point assignment is not dependent on statistical parameters and is therefore independent of the normal distribution restrictions that limit common classification schemes. Rather than use mid-range values alone for characterization, we have used eight additional histogram positions, the appropriate vegetative indices as defined by lag point definition and other user defined ratios.

Our spectral, frequency based classification technique for a grouped set of pixels works with a vector definition for area. Features to be classified are outlined or digitized and selected within a vector based program. Training sites need not be equal in area to unclassified portions of the image, but they must be representative of the category or class. Only those areas outlined and selected are classified..

Visual evaluations are unable to consistently measure and quantify small differences in color. This leads to less precise color quantification and generally limits color ratings to whole number intervals. Linear relationships between visual ratings and data from histograms of the red, green, and blue bands on the same plots can be used to predict new computer enhanced ratings. The computer-enhanced visual ratings consistently had a higher probability of detecting differences between treatments. This increase in statistical

precision was also accomplished without violating the assumptions for homogeneity of variance that visual ratings routinely violate. While more precise and objective than standard ratings, computer enhanced visual ratings gave similar rankings. Because of this statistical precision, computer-assisted ratings were used as a standard by which to measure accuracy for supervised and unsupervised classifications.

Supervised classification was accomplished by developing regression equations. Values for all plots can be predicted given visual measurements of a subset of plots. Statistical precision increases with increasing numbers of training sites in the supervised classification. Predictions made by regression from 18 training sites consistently had a higher probability of detecting differences between treatments than visual ratings. Selecting training sites to include the full range of required values further increased precision. Twelve training sites might be used at a minimum but 18 training sites increase the probability of a representative sample with fewer errors in prediction.

Unsupervised classification requires only a range of color ratings to provide precise predictions of turf color. Rating of plots is purely objective and dependent only on defined histogram values and the resultant statistical patterns. A principal component transformation allows for the selection of the first principal component that describes most of the variability between lag points for red, green, and blue histograms. The range of values is re-scaled to that which is appropriate to rating of the turf.

Unfortunately, unsupervised classifications were inconsistent. Although the treatment mean color rankings are very similar for visual ranking and unsupervised classifications in all three trials, the overall visual and unsupervised color ratings are not strongly associated with each other in Trial 2. These dissimilarities may be attributed to the spectral characteristics of the image.

The Trial 2 color band characterizations for the whole image have no distinct mid-range value in the red band, relatively high minimum brightness values in all three bands and distinct or separable color brightness values for each band. The principal component

transformation effectively separated the color bands while eliminating the redundancy. The 2nd principal component had a higher R^2 for the relationship with the visual ratings than the 1st principal component (data not shown). Trial 3 had a very narrow distribution of brightness values on the low end of the brightness scale and skewed distributions. Low image contrast or narrow distributions of brightness values (DN or digital number values) increases the difficulty in discrimination by lag point definition on the frequency distribution. A wide the range of DN values in all bands and low albedo (relatively high frequencies and low minimum brightness values) may provide for better utilization of principle component procedures. Stretching of the histogram brightness values in all three color bands before analysis may provide for minimum redundancy and a high correlation between the first principal component and the visual ratings.

Use of a color spectra photometer for radiometric error correction on the day and time of digital color ranking for all plots within the trial would be unrealistic for either classification. The photometer can be used for normalization by calibration with ground targets or *in situ* biophysical measurements for removal of atmospheric attenuation. If calibrated for the range of possible rankings, the photometer could be used for calculating a mean visual ranking within a plot or for calculating an error matrix to determine omission and commission error within each of the classification schemes.

The choice for classification in order of precision would be computer-assisted classification as first choice, then supervised classification, unsupervised classification and finally visual rating. The robustness of color classifications suggest relationships between spectral and spatial characteristics of a full color image to the biophysical characteristics of turf. It may be possible to define color relationships for other crop systems to characterize parameters measured such as yield components, disease, pesticide efficacy and soil properties.

BIBLIOGRAPHY

Baker, J.R., S.A. Briggs, V. Gordon, A.R. Jones, J.J. Settle, J.R.G. Townshend and B.K. Wyatt. 1991. Advances in classification for land cover mapping using SPOT HRV imagery. International Journal of Remote Sensing 12(5): 1071-1085.

Blinn, C.R., A. Lyos and E.R. Buckner. 1988. Color aerial photography for assessing the need for fertilizers in Loblolly Pine plantations. Southern Journal of Applied Forestry 12:270-273.

Botkin, D.B., J.E. Estes, R.M. MacDonald and M.V. Wilson. 1984. Studying the earth's vegetation from space. Bioscience 34(8): 508-514.

Cetin, H. and D.W. Levandowski. 1991. Interactive classification and mapping of multi-dimensional remotely sensed data using n-dimensional probability density functions (nPDF). Photogrammetric Engineering and Remote Sensing 57(12): 1579-1587.

Collins, J.B. and C.E. Woodcock. 1996. An assessment of several linear change detection techniques for mapping forest mortality using multitemporal Landsat TM data. Remote Sensing of Environment 56: 66-77.

Dobson, J.E. 1993. Commentary: A Conceptual Framework of integrating Remote Sensing. Photogrammetric Engineering and Remote Sensing 59(10):1491-96.

Dungan, J., L. Johnson, C. Billow, P. Matson, J. Mazzurco, J. Moen and V. Vanderbilt 1996. High spectral resolution reflectance of Douglas Fir grown under different fertilization treatments: Experimental design and treatment effects. Remote Sensing of Environment 55: 217-228.

Dwivedi, R.S. 1996. Monitoring of salt-affected soils of the Indo-Gangetic alluvial plains using principal components analysis. International Journal of Remote Sensing 17(10): 1907-1914.

Erol, H. and F. Akdeniz. 1995. A statistical approach for ground cover modelling according to the spectral brightness. International Journal of Remote Sensing 16(9): 1599-1616.

Estes, J.E. 1992. Remote Sensing and GIS Integration : Research needs status and trends. ITC Journal 1992(1): 2-10.

Everitt, J.H., D.E. Escobar, R. Villarreal, M.A. Alaniz, and M.R. Davis. 1993. Integration of airborne video, global positioning system and geographic information system technologies for detecting and mapping two woody legumes in rangelands. Weed Technology 7:981-987.

Fisher, P.F. and S. Pathirana. 1990. The evaluation of fuzzy membership of land cover classes in sub zones. Remote Sensing of Environment 34: 121-132.

Franklin, S.E. and B.A. Wilson. 1992. A three-stage classifier for remote sensing of mountain environments. Photogrammetric Engineering and Remote Sensing 58(4): 449-454.

Friedkin, W., T.L. Righetti and T. Cook. 1996. Digital analysis of remotely sensed images for evaluating color in turfgrass. Manuscript in process. 19 pgs.

Galvao, L.S., I. Vitorello and W.R. Paradella. 1995. Spectroradiometric discrimination of laterites with principal components analysis and additive modeling. Remote Sensing of Environment 53: 70-75.

Gong, P. and P. Howarth. 1992. Frequency based contextual classification and gray level vector reduction for land use identification. Photogrammetric Engineering and Remote Sensing 58(4): 423-27.

Grossman, Y.L., S.L. Ustin, S. Jacquemoud, E.W. Sanderson, G. Schmuck and J. Verdebout. 1996. Critique of stepwise multiple linear regression for the extraction of leaf biochemistry information from leaf reflectance data. Remote Sensing of Environment 56: 182-193.

Harding, P.J. and C.N. Thomson. 1992. Fast nearest neighbor classification methods for multispectral images. Professional Photographer 44(2): 191-201.

Harris, N.R., T.L. Righetti and D.E. Johnson. 1995. Technical note: Monitoring rangelands and associated riparian zones with blimp borne cameras. Manuscript in Process. 11 pgs.

Hay, G.J., K.O. Niemann and G.F. McLean. 1996. An object-specific image-texture analysis of h-resolution forest imagery. Remote Sensing of Environment 55: 108-122.

Hoffbeck, J.P. and D.A. Landgrebe. 1996. Classification of remote sensing images having high spectral resolution. Remote Sensing of Environment 57: 119-126.

Huete, A.R., R.D. Jackson and D.F. Post. 1985. Spectral response of a plant canopy with different soil backgrounds. Remote Sensing of Environment 17:37-53.

Jackson, P.L., and G.G. Gaston. 1994. Digital enhancement as an aid to detecting patterns of vegetation stress using medium-scale aerial photography. International Journal of Remote Sensing. 15:1009-1018.

Jahne, B. 1993. Digital image processing. Springer-Verlag ,New York.

Jain, A.K. 1989. Fundamentals of digital image processing. Prentice Hall, New Jersey, pp. 418-421.

Jensen, J.R. 1996. Introductory digital image processing. Prentice Hall, New Jersey.

Jensen, J.R., and D.L. Toll. 1982. Detecting residential land use development at the urban fringe. Photogrammetric Engineering and Remote Sensing 48(4): 629-643.

Labovitz, M.L., and E.J. Masvoka. 1984. The influence of auotcorrelation in signature extraction - An example from a geobotanical inventory of Cotterbasin, Montana. International Journal of Remote Sensing 5(2): 315-332.

Lark, R.M. 1995a. A reappraisal of unsupervised classification, II: optimal adjustment of the map legend and a neighborhood approach for mapping legend units. International Journal of Remote Sensing 16(8): 1445-1460.

Lark, R.M. 1996b. Geostatistical description of texture on an aerial photograph for discriminating classes of land cover. International Journal of Remote Sensing 17(11): 2115-2133.

Liu, J.G. and J.McM. Moore, 1990. Hue image RGB colour composition. A simple technique to suppress shadow and enhance spectral signature. International Journal of Remote Sensing. 11(8): 1521-1530.

Mahar, H. and M.S. Afifi. 1995. Linear and correlation analysis for computerized identification of categories in Landsat images. International Journal of Remote Sensing 16(12): 2277-2284

Malthus, T.J., and A.C. Madeira.1993. High resolution spectroradiometry: Spectral reflectance of field bean leaves infected by *Botrytis fabae.* Remote Sensing of Environment 45:107-116.

Meyer, M., and L. Werth. 1990. Satellite data: Management panacea or potential problem? Journal of Forestry 88(9): 10-13.

Palmer, J.R. and R.E. Jacobson. 1995. Comparison of the effectiveness of the principal components transform for enhancing contrast between closely similar colours with a method base on system exposure response differences. International Journal of Remote Sensing 16(8): 1541-1555.

Penuelas, J., J.A. Gamon, K.L. Griffin and C.B. Field. 1993. Assessing community type, plant biomass, pigment composition, and photosynthetic efficiency of aquatic vegetation from spectral reflectance. Remote Sensing of Environment 46:110-118.

Penuelas, J., J.A. Gamon, A.L. Fredeen, J. Merino and C.B. Field.1994. Reflectance indices associated with physiological changes in nitrogen- and water-limited sunflower leaves. Remote Sensing of Environment 48:135-146.

Qi, J., F. Cabot, M.S. Moran and G. Dedieu. 1995. Biophysical parameter estimations using multidirectional spectral measurements. Remote Sensing of Environment 54: 71-83.

Ribeiro, O.K., C.G. Crabtree and E.B. Henrickson. 1994. Possible role of multispectral imagery for the detection of stress vectors in apple replant situations. Acta-Horticulturae 363:169-174.

Schalkoff, R. 1992. Pattern recognition: Statistical, structural and neural approaches. New York: John Wiley, 364 pp.

Swain, D.H. and S.M. Davis. 1978. Remote Sensing: The quantitative approach. New York: McGraw Hill, 166-174.

Toler,R.W., B.D. Smith and J.C. Harlan. 1981. From Hand-Held Cameras to Remote Sensing Techniques. Plant Disease 65:25-31.

Wang, F. 1990a. Fuzzy supervised classification of remote sensing images. IEEE Transactions on Geoscience and Remote Sensing 28(2): 194-201.

Wang, F. 1990b. Improving remote sensing image analysis through fuzzy information representation. Photogrammetric Engineering and Remote Sensing. 56(8): 1163-1169.

Wang, F. 1991c. Integrating GIS's and remote sensing image analysis systems by unifying knowledge representation schemes. IEEE Transactions on Geoscience and Remote Sensing. 29(4): 656-664.

Wildman, W.E., R.T. Nagauka and L.A. Lider. 1983. Monitoring spread of Grape Phylloxera by color infrared aerial photography and ground investigation. American Journal of Viticulture 34:83-94.

Wildman, W.E., W. Bowers and L.T. Bettiga. 1992. Aerial photography in vineyard pest, soil and water management. Grape Pest Management. Ag Sciences Publications, Berkely Press pp. 30-35.

Yoder, B.J. and R.E. Pettigrew-Crosby. 1995. Predicting nitrogen and chlorophyll content and concentrations from reflectance spectra (400-2500 nm) at leaf and canopy scales. Remote Sensing of Environment 53:199-211.

Zahn, C.T. 1971. Graph-theoretical methods for detecting and describing gestalt clusters. IEEE Transactions on Computers C-20(1): 68-86.